



Defense capabilities of *Kentrosaurus aethiopicus* Hennig, 1915

Heinrich Mallison

ABSTRACT

Stegosaurus were not built for rapid locomotion. Instead of fleeing from predators, they probably used their spiked tails as ‘thagomizers’ for defense. Kinetic/dynamic modeling in a computer-aided engineering program allows either using prescribed joint motions to determine joint forces or torque input models that deliver accelerations and moment of inertia of the tail tip spikes. Prescribed motion models based on a CAD range of motion analysis of *Kentrosaurus* and motions observed in extant long-tailed reptiles give results consistent with those of models using torque values calculated from detailed CAD reconstruction of muscle cross sections and moment arms. Both indicate that the tail of *Kentrosaurus* was a dangerous weapon, capable of inflicting painful slashing injuries and debilitating penetrating trauma, even on large theropods, across a large portion of its motion range. Continuous rapid motion was at least sufficient for the spikes to slash open the integument or penetrate soft tissues and fracture ribs or facial bones, while aimed whiplash blows may have had sufficient energy to fracture sturdy longbones.

Heinrich Mallison. Museum für Naturkunde - Leibniz Institute for Research on Evolution and Biodiversity at the Humboldt University Berlin, Berlin, Germany. heinrich.mallison@gmail.com

KEYWORDS: biomechanics; kinetic/dynamic modeling; stegosaur; defense behavior

INTRODUCTION

It has long been theorized that armored dinosaurs, especially stegosaurus, used their tails for defense, swinging them at attackers (e.g., Marsh 1880; Lull 1910; Bakker 1986). Other researchers claimed that this was impossible, because of supposedly insufficient mobility (Gilmore 1914; Hennig 1925; Janensch 1925). However, a plethora of stegosaur spikes with their tips broken off and with callus growths indicate that forceful collisions between stegosaur tails and other objects were not

rare occurrences. Of a sample of 51 stegosaur spikes from the Morrison Formation of North America, about 10% showed broken tips (McWhinney et al. 2001; Carpenter et al. 2005). For the African genus *Kentrosaurus* Hennig, 1915 from the Tendaguru Formation of Tanzania (Hennig 1915) the ratio is unknown, because most material is lost or destroyed (Mallison 2011). However, Hennig (1925, table on p. 232) lists a surprisingly large number of specimens for which the maximum length can either not be given, or only estimated. These missing data may indicate that a significant

PE Article Number: 14.2.10A

Copyright: Palaeontological Association July 2011

Submission: 23 September 2010. Acceptance: 18 February 2011

Mallison, Heinrich. 2011. Defense capabilities of *Kentrosaurus aethiopicus* Hennig, 1915. *Palaeontologia Electronica* Vol. 14, Issue 2; 10A:25p;
palaeo-electronica.org/2011_2/255/index.html

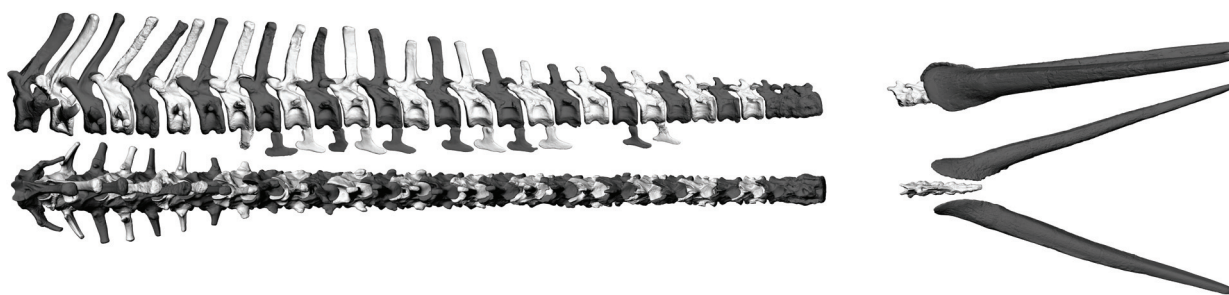


Figure 1. High resolution laser scan digital 3D files of MB.R.4800.6-32, the nearly complete tail (caudals 1 through 29, 27-29 coossified) of the lectotype of *Kentrosaurus aethiopicus* Hennig, 1915, from quarry 'St', Tendaguru, Tanzania. Tail tip MB.R.4801.1-6 (coossified) from same locality may also belong to lectotype (Hennig 1925). MB.R.4842 (left) and MB.R.4843 (right) spikes from same quarry, definitively not part of lectotype, and probably not tail tip spikes, but second to last spike pair. Gap between MB.R.4800.32 and MB.R.4801.1 according to estimate of missing caudal number by Janensch (1925). Length of left spike MB.R.4842, measured as maximum possible value in dorsal view, 713 mm. 1. lateral view, 2. dorsal view.

percentage showed broken tips similar to those of American stegosaur spikes, but it is unclear which of these spikes are really tail tip spikes of *Kentrosaurus* and which were located further anteriorly. Carpenter et al. (2005) detailed the impact-related pathologies on stegosaur tail spikes and an exceptional find, which was a pathological caudal of *Allosaurus* Marsh, 1877 (Marsh 1877a) that apparently was struck at high velocity by a stegosaur spike tip. The impact destroyed part of the transverse process and the tip of the spike pierced the neural spine (Carpenter et al. 2005, figure 17.2). Carpenter et al. (2005) also assessed the forces involved, concluding that the tail of *Stegosaurus* Marsh, 1877 (Marsh 1877b) was strong enough to cause the damage. They also detailed two different methods for calculating the forces involved in causing damage to the spikes, concluding that both slashing and spearing actions took place. The forces involved both in slashing and spearing were sufficient to break spikes in the manner observed in the fossil record and sufficient to cause the damage to the *Allosaurus* vertebra (Carpenter et al. 2005). To date, this report remains the single published detailed biomechanical analysis of stegosaur tails.

The other main group of thyreophorans, ankylosaurs, has seen barely more attention. Coombs (1978, 1979) studied their myology in detail and speculated that the tail was occasionally used to club predators, but did not attempt to assess forces and accelerations involved. Maleev (1952) regarded the tail club as a 'mace', and Arbour (2009) investigated tail mobility and impact forces in detail, distinguishing three categories of caudal vertebrae in ankylosaurs with three different functions: free vertebra form the flexible base of the tail,

handle vertebra form a rigid club, and a transitional vertebra lies between the two. In the derived stegosaur *Stegosaurus*, the tail may have been functionally sectioned not by difference in vertebra shape, but by the large osteoderm plates, which inhibited motion so that five near-rigid sections were formed (Carpenter 1998; Carpenter et al. 2005). This condition is a marked contrast to basal thyreophorans such as *Scelidosaurus* and stegosaurs other than *Stegosaurus*, where a functional partitioning is, where the tail is known, absent because there were no osteoderms with a large anteroposterior extension present on the tail (e.g., *Huayangosaurus* Dong et al., 1982; [Maidment et al. 2006]; *Kentrosaurus* [Hennig 1925; Mallison 2010a]). For some species the tail is insufficiently known (e.g., *Miragaia* Mateus et al., 2009). In *Kentrosaurus*, the caudal vertebrae change significantly in shape, with the neural spines of the anterior caudals inclined posteriorly, those in the middle part of the tail sub-vertical, and those in the distal third hook-shaped and inclined anteriorly (Hennig 1925; Mallison 2010a, figure 5). The change is gradual, and lateral and dorsal mobility between neighboring vertebrae is unaffected and remains constant throughout the tail (Figure 1.1; Mallison 2010a, figures 5, 6, 9, 10).

The use of the tail as a weapon is common in extant reptiles, e.g., monitor lizards (Holland 1915), lacertilians (Carpenter 1961; Milstead 1970) and crocodylians (e.g., Pooley and Gans 1976). All crocodylians use vigorous swings of their tails to reverse the direction their snout points in, but alligators especially use powerful swipes of their tails to strike approaching antagonists (or other objects perceived as such; personal observation). Mammals usually do not have long, thick tails, so that

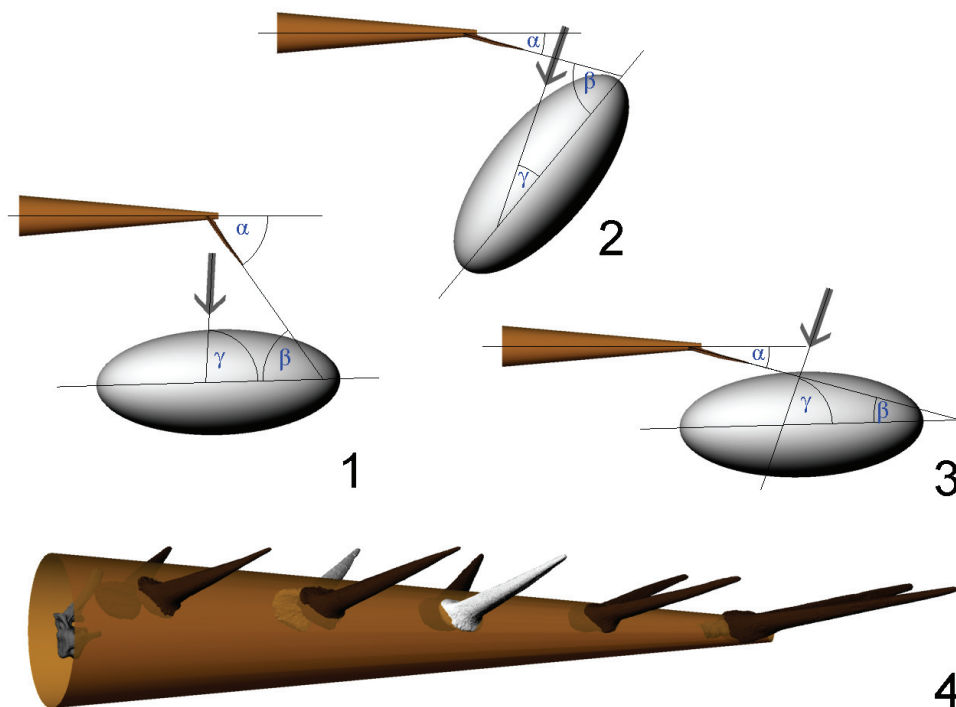


Figure 2. Impact geometries (1-3) and tail reconstruction of *Kentrosaurus aethiopicus* Hennig, 1915 (4). 1. penetrating impact, 2. slashing impact, 3. blunt impact. Arrow = direction of travel of spike at impact, α = angle between long axes of spike and tail, β = angle between long axis of spike and surface of target (long axis of target used as proxy), γ = angle between direction of travel of spike and surface of target (long axis of target used as proxy). Note how large values for α are required for a penetrating impact, because the direction of travel of the spike is generally limited to a circle around the tail base. Small values for β make blunt impacts likely. 4. likely distribution and orientation of tail spikes (high resolution laser scan digital 3D files of MB.R.4836- 4843, from left to right), based on description and figures in Hennig (1925). Light grey bones are digital mirror images of contralateral side. Tail modeled as truncated cone over high resolution laser scan digital 3D files of MB.R.4800.6 (caudal 1 of lectotype) and MB.R.4801-6 (coossified tail tip vertebrae). All fossils from quarry 'St', Tendaguru, Tanzania, all spikes not part of lectotype and not found in association.

other body parts are employed as weapons. Horns and antlers, e.g., usually are used in intraspecific fights between males (see, e.g., Geist 1971; Clutton-Brock 1982) and may be involved in resource competition between female ruminants (Roberts 1996). However, glyptodonts apparently used their tails (some of them club shaped) in intraspecific fights, delivering blows sufficiently strong to fracture and dent the opponent's carapace (Alexander et al. 1999). Considering everything, it seems highly likely that *Kentrosaurus* employed its tail as an active weapon, very likely for defense against predators, and potentially also for intraspecific fights.

For any modeling of a potential tail strike, the geometry of the impact is of importance. Three types of impacts must be distinguished: penetrat-

ing, slashing, and blunt. In penetrating impacts the spike tip works like a spear tip, for slashing it works like a scimitar, and in blunt impacts the spike acts like a club or mace. The impact types differ in the angles between the spike's long axis, its direction of travel, and the target surface. A deeply penetrating impact can occur only if a spike moves subparallel to its long axis and roughly perpendicular to the target surface (Figure 2.1). Large angles between the spike's long axis and its direction of travel lead to slashing impact when the spike travels at a shallow angle compared to the target (Figure 2.2) and to a blunt impact if the spike travels roughly toward the target (Figure 2.3). The distance between stegosaur and target also plays an important role and can determine if a slashing

impact on one part of the target's body or a blunt impact on another part occurs.

The tail spikes of *Stegosaurus* (e.g., Marsh 1880, pl. X; McWhinney et al. 2001, figure 7.1; Carpenter et al. 2005, figure 17.3) have a form intermediate between a spear (causing penetrating trauma) and a club (causing blunt trauma). The sharp tips are suitable for slashing and for easily penetrating soft tissues, but the conical form means that deeper penetration pushes a much larger cross section into the opponent, increasing the energy needed to increase penetration depth significantly. If an impact occurs at a shallow angle to the long axis of the spike, the contact area is large, as with a club, and penetration requires a much higher impulse. Compared to the North American genus, the distal tail spikes of *Kentrosaurus* are slimmer, being only about half as wide at the base, proportionally (Hennig 1915, figure 3, 1925, figure 54). The distribution of osteoderms on the body of *Kentrosaurus* is not entirely clear, with only a few found semiarticulated (Hennig 1925; Janensch 1925). Fortunately, the shape of the most distal spike pair is known with certainty, because one pair was found articulated with five distal caudal vertebrae (MB.R.3803; Hennig 1925; Figure 3). The spikes supposedly show flattening on the ventral side (Hennig 1925), but in fact have been crushed and deformed by taphonomic processes. Very likely they had a roughly elliptical cross section, and the ends of the major diameter showed small keels (Figure 3.2). This shape is highly reminiscent of a spear tip and suggests that penetrating or slashing impacts were easier to achieve for *Kentrosaurus* than for *Stegosaurus*.

However, the spikes on the tail tip apparently angled out from the long axis of the tail by only a small angle, as indicated by the angle between their bases and shafts. The angles may be as low as 20° (Hennig 1925), while spikes positioned further anteriorly showed increasingly larger angles and stouter form (Figure 2.4). Together, the arrangement and shape change of the spikes may indicate that the tail tip functioned primarily as a slashing weapon, with the occurrence of deeply penetrating strikes unlikely, while the slower moving spikes further anteriorly served mostly as defensive pikes, shaped to penetrate a predator that tried to attack the tail base. For this purpose, the spikes would need to stick out steeply, pointing their ends at the target. On the other hand, the spikes of MB.R.3803 may today be angled much more strongly than they were in life, and the angle

between base and spike shaft may not be indicative of the true orientation of the spike. The tail tip of *Kentrosaurus* may then have been highly similar in overall appearance to that of *Stegosaurus*, in which the spikes stood out at nearly a 45° angle (Carpenter 1998, figure 3). Even a more laterally directed orientation is possible, because decay of soft tissues before complete burial of the articulated finds (e.g., the *Stegosaurus stenops* specimen shown in Carpenter [1998, figure 3]) could have led to the spikes being folded closer to the vertebral column than during life.

Overall, geometry appears to indicate that blunt impacts of the tail tip spikes were most likely, with slashing impact also occurring, while deep penetrating trauma was rare. The large number of broken spikes (McWhinney et al. 2001; Carpenter et al. 2005), in contrast, may indicate that the above assessment of the geometry is wrong, and that the spikes may have "hooked into" the target's body. Therefore, all types of impacts must be taken into account when assessing stegosaur defense behavior.

Besides the geometry of the impact, the speed of the tail tip is the main factor determining the damage a tail strike can cause. It depends on the tail's motion geometry and on the forces that the musculature can generate, which in turn depend directly on the available muscle cross section. Previously published reconstructions of dinosaur tail muscle cross sections usually differ significantly from the tail morphology of extant monitor lizards and alligators, as shown, among others, by Persons (2009) in a dissection study. A detailed assessment of tail volume and the influence of its reconstruction on COM position by Allen et al. (2009) found, for non-avian sauropsids, on average 158% mediolaterally, 133% dorsally, 186% ventrally, 91% dorsal diagonally, and 112% ventral diagonally greater dimensions in reality than in a simple, bone-determined elliptical model. Allen et al. (2009) found that their most detailed and realistic models closely approximated body mass, whereas the elliptical models underestimated total body mass by nearly 14%.

In their reconstruction of dinosaur tail muscles Carpenter et al. (2005) limited the lateral and dorsoventral extent of the musculature to the tips of the supporting bony structure (i.e., the tips of the transverse processes, the neural spine, and the haemapophysis) for *Allosaurus*, and created a roughly elliptical cross section based on these limits, the equivalent of the elliptical, bone-determined models of Allen et al. (2009). In *Stegosaurus*, the

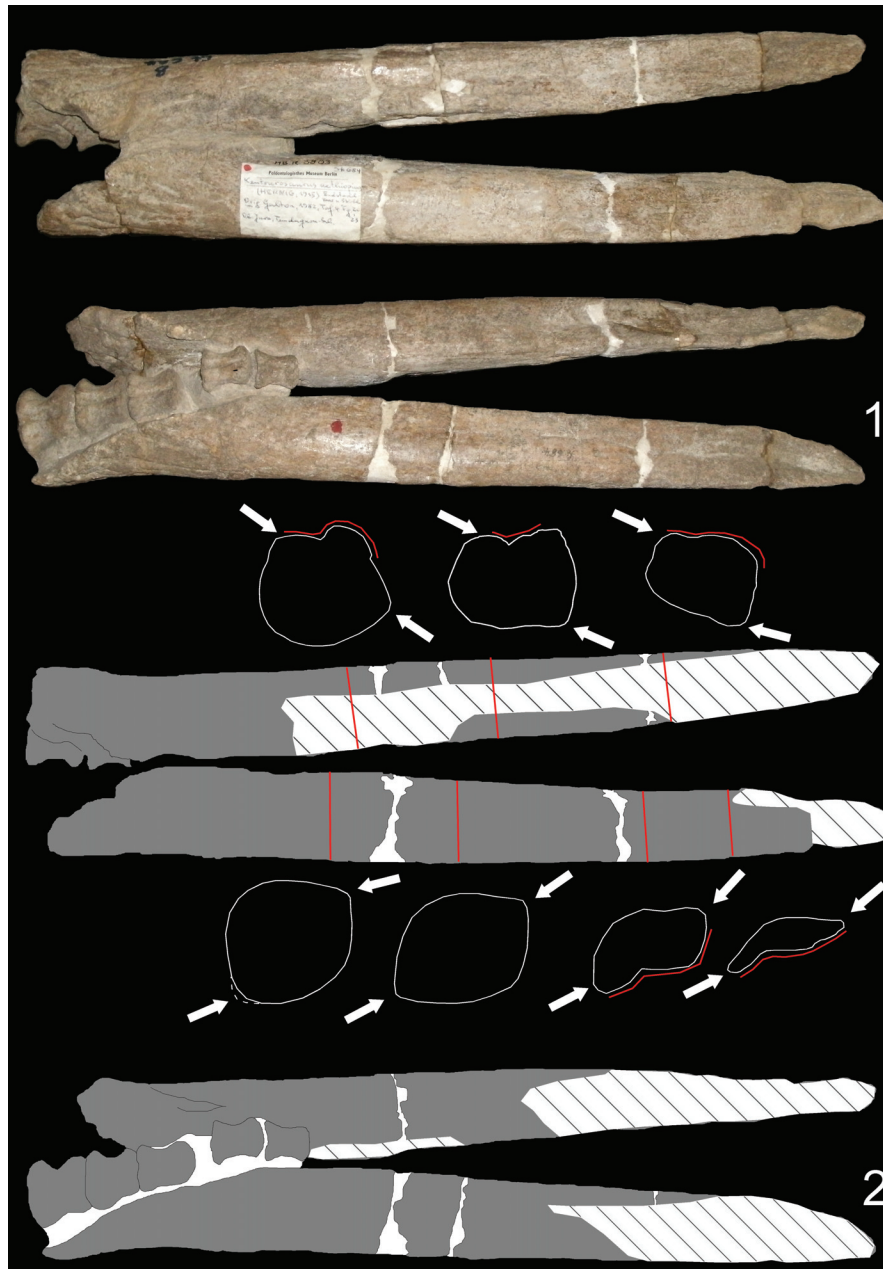


Figure 3. MB.R.3803, a pair of tail tip spikes and five distal caudal vertebrae of the stegosaur *Kentrosaurus aethiopicus* Hennig, 1915, from quarry 'St', Tendaguru, Tanzania. Length of right spike 44.6 cm. 1. top: dorsal view, bottom: ventral view. 2. Scheme showing areas with significant damage (massive surface erosion and/or crushing) visible on the bone surface (hatched) and cross sections (positions indicated by red lines). Red curves parallel to cross sections show damaged areas, white arrows point at keels. Note the small size of the keels and that an overall convex surface persists where the bone is undamaged.

expanded transverse processes force the *m. ilio-caudalis* into a lateral position. The muscle cannot be limited to the extent of the transverse processes, because there would not be any room for it. Carpenter et al. (2005) chose to create a narrow high-oval tail cross section (reproduced in Figure

4.6), in which the *m. caudofemoralis* attaches only to the ventral side of the transverse processes, but not to the haemapophysis, and the *mm. articulospinalis* and *spinalis* are limited to the lateral side of the neural spine. In these reconstructions, the bone cross section area amounts to 21% (*Allosau-*

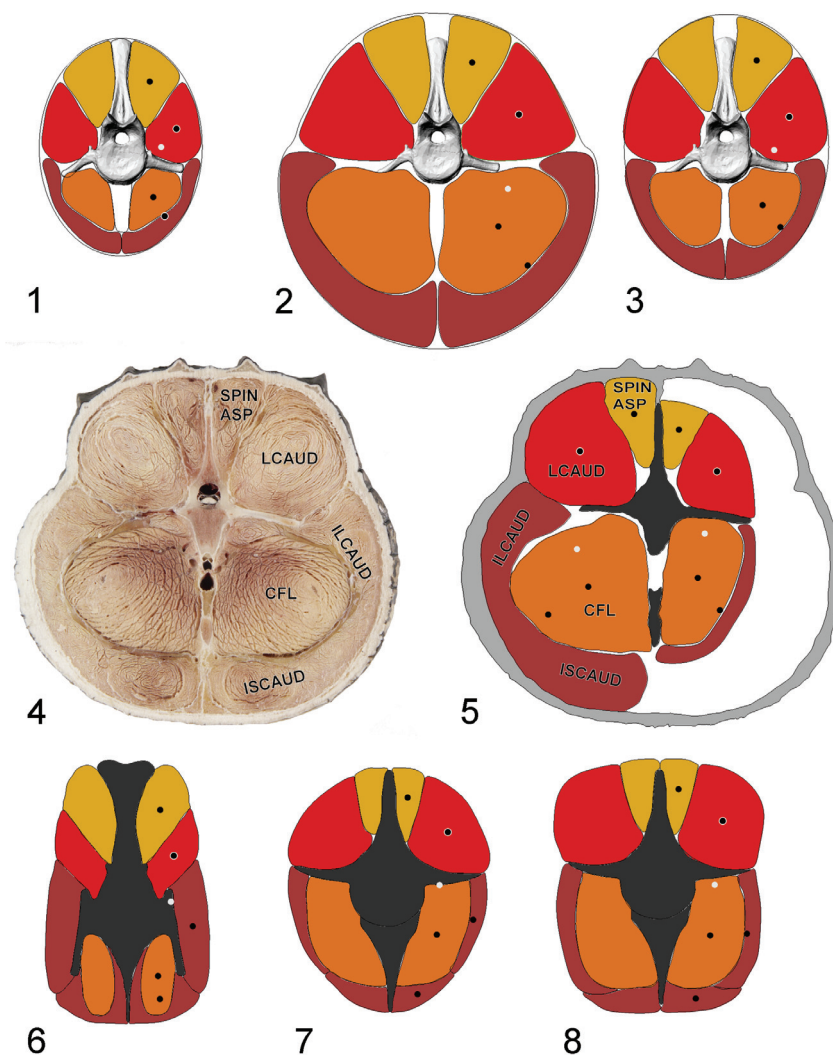


Figure 4. Tail muscle cross section reconstructions and photograph. Black dots denote individual muscle area centroids (moment arms), light grey dots denote centroids for entire half of tail. 1. 'slim', 2. 'croc' and 3. 'medium' muscle cross section reconstructions for *Kentrosaurus aethiopicus* at the base of the tail. Note shift of centroids with changing muscle areas. 4. photograph of section of the base of the tail of *Alligator mississippiensis* provided by D.R. Wilhite (see text for further explanations). 5. tracing of *Alligator* as in 4 on the left, and reconstruction following typical dinosaur reconstructions on the right. Integument of *Alligator* photograph is traced on the right also, to highlight the difference in cross sections between the living animal and the typical method of reconstruction. 6, 7, 8. tracings of previous reconstructions of (6) *Stegosaurus* from Carpenter et al. 2005 and (7 and 8) ankylosaurs from Arbour (2009). All figure parts scaled to approximately the same vertebra size. Height of *Kentrosaurus* caudal 278 mm. Abbreviated muscle names: ASP = m. articularis spinalis, CFL = m. caudofemoralis longus, ILCAUD = m. iliocaudalis, ISCAUD = m. ischio-caudalis, LCAUD = m. longissimus caudae, SPIN = m. spinalis.

rus) and 28% (*Stegosaurus*) of the muscle cross section areas as determined by tracing the drawings in Rhinoceros®. In contrast, tracing of several *Alligator* tail section photographs resulted in values between 6.0 and 6.4% (Figure 4.4-4.5). Arbour (2009) used the same limits as Carpenter et al. (2005) for her model of an ankylosaur tail (reproduced in Figure 4.7; note that Arbour [2009] recon-

structed m. articularis spinalis and spinalis as m. transversospinalis), but also published a second, more muscular reconstruction (reproduced in Figure 4.8), in which the muscles bulge significantly beyond the bones. Arbour (2009, figure 9) stated that this led to an increase of muscle cross section by 43%. However, tracing of Arbour's (2009, figure 9) original figure in Rhinoceros 4.0 shows that the

actual increase is close to 30%. The slim model by Arbour (2009) has 24% bone cross section area, while the more muscular model has 19%. Clearly, new modeling attempts must include more muscular model versions as well.

Here, I present the results of NASTRAN-based computer-aided engineering (CAE) modeling of tail motions of *Kentrosaurus*, which allow estimating the tail tip speeds and impact forces across the entire motion range of the tail in higher detail than the mathematical methods of Carpenter et al. (2005), using musculature reconstructions based both on previous methods, on data from extant alligators, and an intermediate version.

Institutional Abbreviations

DMNS, Denver Museum of Nature and Science, Denver (US)

MFN, Museum für Naturkunde – Leibniz-Institut für Evolutions- und Biodiversitätsforschung an der Humboldt-Universität zu Berlin, Berlin (Germany) Collection numbers MB.R.####

NMS, Naturmuseum Senckenberg, Frankfurt (Germany)

SMA, Sauriermuseum Aathal, Aathal (CH)

MATERIAL

The nearly complete composite skeleton of *Kentrosaurus aethiopicus* Hennig, 1915 from the Late Jurassic of Tendaguru, Africa, on exhibit in the MFN, was high-resolution laser scanned bone by bone by Research Casting International (RCI; www.rescast.com) during the museum renovation in 2007. Here, the digital skeletal mount by Mallison (2010a) is used. The tail of this mount (Figure 1; Mallison 2010a, figure 5) is nearly complete and is from one individual (see Mallison 2011). Stegosaur mounts in the DMNS, SMA, and NMS were used for comparison.

For muscle reconstructions, I used cross sections of a healthy *Alligator mississippiensis* (Daudin, 1802) of ~ 1.4 m total length. The animal was perfused and sectioned into 62 slices by D. Hillmann (Louisiana State University School of Veterinary Medicine), and high-resolution color photographs (example shown in Figure 4.4) were taken by D.R. Wilhite (Auburn University College of Veterinary Medicine), who graciously provided them for this project. Twenty of the slices stem from the base and middle part of the tail; the distal part was not sectioned. Each slice was photographed in anterior and posterior view, so that the

extents and paths of major muscles are well documented.

METHODS

Tail Musculature Reconstruction

The tail muscles of *Kentrosaurus* were reconstructed using the terminology employed in Carpenter et al. (2005). As in Arbour (2009), extant crocodylians were chosen as a guide, because crocodylians are the sole extant archosaurs with long and muscular tails.

Muscle paths of *Alligator* and other extant tailed reptiles were taken from the literature (Romer 1923a, 1927; Gasc 1981; Frey et al. 1989; Cong et al. 1998) and dissection data. On the basis of these reports, combined with muscle reconstructions of closely related taxa (Coombs 1979; Carpenter et al. 2005; Arbour 2009) and other dinosaurs (e.g., Romer 1923b), the major tail muscles of *Kentrosaurus* were reconstructed in cross section at the base of the tail immediately distal to the cloaca and at roughly one-third the tail length (Figure 1). These two points were chosen because the force produced in the basal part of the tail influences tail swing speeds the most, and because the size of the vertebrae, which correlates with that of the soft parts, decreases almost linearly along the tail, so that distal parts can be modeled by scaling down the anterior parts. In order to determine muscle diameters, the cross section photographs of the alligator tail were imported into McNeel Associates Rhinoceros 4.0 NURBS Modeling for Window©, and the muscle and bone outlines traced. Surfaces were created to fill in the muscle outlines, so that the cross section areas as well as area centroids could be directly calculated in Rhinoceros 4.0. Because data from dissection and from the cross section photographs disagrees with the common practice to limit soft tissues to the extent of the bones (tips of transverse processes, neural spines, haemapophyses as in, e.g., Paul 1987; Christiansen 1996; Carpenter et al. 2005; Arbour 2009) three versions were created. The first (henceforth 'slim'; Figure 4.1) follows the literature and assumes that the soft tissues form an ellipse with the tips of the neural arch and the haemapophysis determining the long axis, and the tips of the transverse processes forming the short axis. The second model ('croc'; Figure 4.2) has axes proportionally as much longer than the extent of the bone as the average values of the measurements taken on the alligator cross section photographs. However, the model is not proportionally

equivalent to the alligator, but has somewhat smaller muscle cross section areas, because the alligator's muscles bulge out, while those of the model do not. This model conforms roughly to the general extent of the tail muscles in extant reptiles as determined by dissection by Persons (2009) and via digital 3D reconstruction based on CT data by Allen et al. (2009). The third model ('medium'; Figure 4.3) has an elliptical shape like the 'slim' model, but axes lengths are the arithmetic average of the 'slim' and 'croc' models. The alligator section used for the muscle reconstruction at the base of the tail is shown in Figure 4.4, the tracing of it in Figure 4.5, combined with a muscle reconstruction for the alligator following the dinosaur muscle reconstruction paradigm (elliptical model). *Mm. ischiocaudalis* and *iliocaudalis* were not separated in the tracings and reconstructions, because their contact line in the *Alligator* cross sections is often difficult to determine exactly. Their exact sizes relative to each other are not of importance for the models computed here. Also, at the very base of the tail of the alligator, a part of the *m. iliocaudalis* runs between the transverse process and the *m. caudofemoralis*, which was here counted as part of the *m. caudofemoralis* to achieve consistency with the reconstructions from the literature. For comparison, tracings of the reconstructions of *Stegosaurus* in Carpenter et al. (2005) and the slim and the muscular version for ankylosaurs in Arbour (2009) are shown in Figure 4.6-4.8, scaled to the same vertebral size.

The torque values T each muscle could produce were calculated based on these reconstructions:

$$T = A * P * l \quad (1),$$

with A being the cross section area, P the specific tension, and l the moment arm of the muscle. The moment arms were determined by measuring the horizontal distance of the area centroids of the muscles from the sagittal plane in the CAD program. Values for specific tension vary widely in the literature, from as low as 15 N/cm² to as high as 100 N/cm² (e.g., Fick 1911; Franke and Bethe 1919; Barmé 1964; Langenberg 1970; Maganaris et al. 2001). Carpenter et al. (2005) use two values to bracket the probable range, 39 N/cm² and 78 N/cm², based on data in Ikai and Fukunaga (1968). Arbour (2009) used 20 N/cm², based on studies on humans and cats. A detailed study on the *m. quadriceps* group in humans found values between 50 N/cm² and 60 N/cm² (O'Brien et al. 2010). Marx et

al. (2006) report values between 25 N/cm² to 45 N/cm² from a wide size range of animals, including values of ~ 35 N/cm² from a rhinoceros.

At the top end of the spread reported in the literature, values over 70 N/cm² stem mainly from older literature and can be discounted because of methodological problems. The remaining variation of values is partly explained by various physical, methodological and biological reasons (Bottinelli and Reggiani 2000). Also, the joint angles at which the measurements of moment arms are made strongly influence the estimated specific tension (Winter and Challis 2003). Force production of a muscle depends also on the speed of the contraction, with slow continuous contraction allowing higher values than rapid contraction (Alexander et al. 1999). Since tail swinging involves relatively slow contractions, the values of 20 N/cm² and 50 N/cm² are used here, as they bracket the most likely range. 39 N/cm² and 78 N/cm² are used to create comparability to Carpenter et al. (2005). The former value is close enough to the middle of the 20-50 N/cm² range that results using it can be regarded as the likely upper end of the best estimate range. Table 1 lists the muscle cross section areas and torques for the reconstructions at the base of the tail.

This method for estimating available torques is a gross simplification, ignoring important details such as the internal structure of the muscles (straight-fibered or pinnate, which determines if there is a difference between geometrical and physiological muscle cross section) or the complex relationship between muscle fiber length, muscle contraction, and force production. Highly detailed musculoskeletal modeling in a dedicated program (e.g., SIMM, see Delp and Loan [1995, 2000]; Hutchinson et al. [2005]) could take these and other factors into account, but the gain in accuracy may well be negated by the inaccuracies necessarily included in the estimates of muscle mass, motion range, spike position, and angle and specific tension. A detailed sensitivity analysis covering all these factors is beyond the scope of this work.

CAD Model Creation

The high-detail 3D model was created in Rhinoceros 4.0® on the basis of NURBS ellipsoids, which were deformed via control point (node) editing. Spikes and plates were created as separate elements (Figure 5.1-5.4). Of the tail three additional versions were created (Figure 5.5) corre-

Table 1. Measured and reconstructed muscle cross section areas, muscle moment arms and maximally available torques at the base of the tail in *Alligator* and three versions of the *Kentrosaurus* reconstruction. Torques were calculated for four different specific tension values between 20 N/cm² and 79 N/cm². Abbreviated muscle names: ASP = m. articularis, CFL = m. caudofemoralis longus, ILCAUD = m. iliocaudalis, ISCAUD = m. ischiocaudalis, LCAUD = m. longissimus caudae, SPIN = m. spinalis. *Alligator* sections are without scale and here scaled to approximate same vertebra height as *Kentrosaurus* caudal, 278 mm.

muscle	area (m ²)	lever arm (m)	force @ 20 N/cm ²	(N) @ 39 N/cm ²	@ 50 N/cm ²	@ 78 N/cm ²	torque @ 20 N/cm ²	(Nm) @ 39 N/cm ²	@ 50 N/cm ²	@ 78 N/cm ²
<i>Alligator</i>										
ASP + SPIN	0.011	0.046	2200	4290	5500	8580	101.2	197.3	253	394.7
LCAUD	0.038	0.149	7600	14820	19000	29640	1132.4	2208.2	2831	4416.4
CFL	0.054	0.122	10800	21060	27000	42120	1317.6	2569.3	3294	5138.6
IL- + ISCAUD	0.0495	0.193	9900	19305	24750	38610	1910.7	3725.9	4776.8	7451.7
sum	0.1525						4461.9	8700.7	11155	17401.4
<i>Kentrosaurus</i> 'croc'										
ASP + SPIN	0.0165	0.065	3300	6435	8250	12870	214.5	418.3	536.25	836.6
LCAUD	0.0305	0.153	6100	11895	15250	23790	933.3	1820.0	2333.3	3639.9
CFL	0.0445	0.114	8900	17355	22250	34710	1014.6	1978.5	2536.5	3957.0
IL- + ISCAUD	0.035	0.169	7000	13650	17500	27300	1183	2306.9	2957.5	4613.7
sum	0.1265						3345.4	6523.5	8363.5	13047.0
<i>Kentrosaurus</i> 'medium'										
ASP + SPIN	0.0125	0.058	2500	4875	6250	9750	145	282.8	362.5	565.5
LCAUD	0.021	0.119	4200	8190	10500	16380	499.8	974.6	1249.5	1949.2
CFL	0.015	0.069	3000	5850	7500	11700	207	403.7	517.5	807.3
IL- + ISCAUD	0.013	0.1	2600	5070	6500	10140	260	507	650	1014
sum	0.0615						1111.8	2168.0	2779.5	4336.0
<i>Kentrosaurus</i> 'slim'										
ASP + SPIN	0.0105	0.054	2100	4095	5250	8190	113.4	221.1	283.5	442.3
LCAUD	0.011	0.1	2200	4290	5500	8580	220	429	550	858
CFL	0.008	0.06	1600	3120	4000	6240	96	187.2	240	374.4
IL- + ISCAUD	0.007	0.081	1400	2730	3500	5460	113.4	221.13	283.5	442.3
sum	0.0365						542.8	1058.5	1357	2117.0

sponding to the three muscle cross section models.

The limbs of the model were sectioned into functional units (e.g., brachium, antebrachium, manus). In the neck, trunk, and tail, one segment should ideally correspond to one vertebra plus soft tissues, as is the case for the initial, detailed model of the tail (Figure 5.5), but this would lead to such a high number of individual bodies to be handled by the CAE program that calculation times would become intolerable. Therefore, a simpler sectioning of the 'slim' tail model was created, dividing the tail into five parts, with the spikes distributed following Janensch (1925), and incorporated into the respective sections (Figures 5.1-5.4). These sections do not correspond to specific points in the tail

(changes in morphology of the caudal vertebrae or in mobility), because the changes in vertebral shape are continuous, and mobility between vertebrae remains constant (Mallison 2010a). The number of segments is a compromise, attempting to keep computing times tolerable (each additional segment doubles computing time) while using a sufficient number of segments to achieve overall similarity between the geometry of the real tail's motion and that of the model. Figure 5.6 shows both the detailed and simplified tail models in a strongly laterally deflected pose in comparison.

Instead of creating similar simplified versions for the 'medium' and 'croc' tail models, the density of the simple model was accordingly increased in the CAE software.

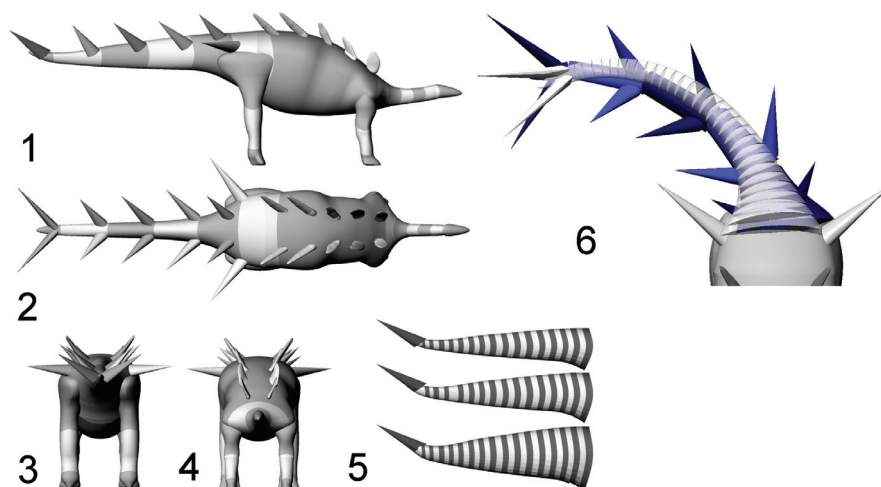


Figure 5. *Kentrosaurus aethiopicus* CAD model in lateral (1), dorsal (2), caudal (3), and cranial (4) views. Zebra stripe coloring highlights the separation into functional sections for the CAE simulation. 5. detailed models of the tail in lateral view. Versions top to bottom: 'slim', 'medium', 'croc'. One section represents one caudal vertebra plus the corresponding soft tissues. 6. Detailed 'slim' model and simplified five-segment model of the tail superimposed, in strong lateral flexion. Note how five segments suffice to roughly similar overall curvature. Total length of the model (snout to tail tip) 4.77 m.

The trunk was split into two parts, one for the sacral region, one for the rest, and the neck was arbitrarily split into five sections.

NASTRAN Modeling

Computer Aided Engineering (CAE) was conducted in MSC.visualNASTRAN 4D© by MSC Corp. and NX 5.0© by Siemens AG. The CAD model parts were imported as *.stl (binary ASCII polygon mesh) files. Because the sole physical property of significance for the simulations presented here is density, all other values such as thermal conductivity, specific heat, and yield stresses were set to the defaults (i.e., those of steel). Mass was adjusted as appropriate by setting a specific density for each individual object, as described below.

Some simulations were conducted by defining joint motions through table or formula input, based on desired results (e.g., orientation per time for a swing across the full arc). Henceforth, these are termed 'prescribed motion' models. They can result in motions that are impossible, e.g., because the required accelerations could not be produced by the available musculature, or because the motion range was exceeded. Therefore, internal (through data derived within the simulation) and external (through comparison to motion range analysis (Mallison 2010a) or further calculations outside NASTRAN) controls were necessary and are

described where appropriate. Other models limited the motion range of joints in the CAE program a priori to the values determined by the range of motion analysis by Mallison (2010a). On the basis of the determined maximum muscle forces and moment arms, joint torques were calculated and used to drive these models, here termed 'torque' models.

Most of the 'prescribed motion' models could be simulated with simple Euler integration, but all 'torque' models required the more detailed and accurate Kutta-Merson integration with variable time steps. The mathematical basics of both methods are described in Fox (1962). Because of the much higher calculation time demands of Kutta-Merson integration, only a limited number of models could be computed.

The detailed tail models with 32 segments, and thus 33 joints (31 between segments, one to anchor the tail to the hip, and one to connect the spikes; Figure 5.5), cannot be computed as 'torque' models, because the required accuracy would result in calculation times upwards of a week per model run. Therefore, the simplified tail version with only five segments was used instead (Figure 5.1, 5.5). This model does not result in an identical overall curvature, but the moment arms are sufficiently similar that it can be used instead of the more detailed tail model, because the uncertainties in all other respect (muscle reconstruction, range

of motion analysis, implicit assumptions in the 3D CAD model, flexion rates of the tail) have a much larger influence on the accuracy of results. The slight inertia differences between the two tail models do not play a significant role.

Mass Estimates and COM Position

Variations of the density of all parts of the CAD model were undertaken, to simulate larger or smaller amounts of soft tissues than those assumed in the three CAD models. The position of the center of mass (COM) was determined in the CAE program.

The fraction of total body weight supported by each pair of limbs is identical to 1 minus the limb pair's proportional distance from the COM (Alexander 1989; see also Henderson 2006). Changes in an animal's posture alter the moment arms of body parts, shifting the position of the overall COM. This change can be tracked in NASTRAN, as well as the lateral accelerations of the entire animal, here measured at the posterior body segment. These tests were run with both the simplified and the detailed tail models.

Several models of tail swings were run with the tail tip impacting a large generic object representing a mid-sized or large predator, to test the effect of impacts on the inertia of the entire animal. The impacts were set to a coefficient of restitution of 0.5, meaning that 50% of the total impact energy is transferred back to the tail, while the other half is consumed in tissue deformation. This value is probably too high and underestimates the stability of the animal.

Continuous Tail Swings

Tail motions were modeled first as 'prescribed motion' models, with continuous accelerations and decelerations in each joint (i.e., the entire tail musculature was assumed to be actively involved in creating the swing), using a simple sinusoid function with a 1 s, 1.5 s and a 2 s period. Crocodiles and alligators as well as large monitor lizards can all move their tail through large arcs in between below 0.3 s for smaller animals and less than 0.5 s for large animals (> 3m body length, pers. obs.), although it is unclear whether these motions involve the full motion range or the maximum possible speed. Flexion per joint was set to 2.5°, 5°, and 6°, with all joints given equal values, because mobility along the tail apparently was constant (Mallison 2010a). Greater values would lead to the tail tip spike hitting the trunk, unless the tail was in an extended position. The required torque at the

base of the tail and the speed of the tail tip in relation to the deflection angle were measured. Additionally, the models were adjusted to achieve the same overall swing times to cover the whole arc, but distribute the applied torque values more evenly. All these models were run without any target for the tail to impact on. This way, it could be determined if a strike missing the target would unbalance the animal.

Whiplash Tail Swings

A sinusoid deflection rate leads to maximum speed at the half-angle (i.e., when the tail is straight). Whiplash actions shift the maximum speed angle and can increase the top speed significantly. Since the mechanics of whiplashes are complex, no attempt was made to calculate ideal motions to create maximum speed or a certain high speed across as large an arc as possible. Rather, simple motions were improved by trial and error. When results showed speeds high enough to cause serious injury to other animals, optimization of the motion was halted.

The high speeds involved in the 'crack' of a bullwhip rely on two basic properties: flexibility and a tapering diameter from the base to the tip (Bernstein et al. 1958). Whip dynamics are described in detail for the tails of diplodocid dinosaurs in Myhrvold and Currie (1997). In principle, to create high speeds at the end of the whip, a wave running down the length of the whip is created by suddenly halting or reversing rotation at the base. The wave gains speed on its way because the constant angular momentum is applied to ever decreasing amounts of mass under an ever shortening radius. The simplest way to create such a motion in the tail of *Kentrosaurus* with a maximum of angular momentum was acceleration of the base of the tail, which acts as the whip handle, starting at maximal lateroflexion and continuing through the entire motion arc, with the osteological or soft tissue stops halting motion suddenly when maximum lateroflexion on the opposing side is achieved. Then, the base of the tail is accelerated in the opposite direction, here using two-thirds of the maximum calculated torque. The more distal joints were similarly accelerated for appropriate intervals into the direction of the swing using the full calculated torque, and then accelerated in the opposing direction using two-thirds of the maximum torque (i.e., as in the continuous swing models the entire tail was assumed to be actively contributing to the motion). Depending on when exactly which joint's direction was reversed, the top speed varied

widely, and the point at which the tail tip achieved this speed was located in different places. No attempts were made to maximize the speeds, or the arc across which it was achieved, but a roughly exponential increase in tail tip speed through the motion was aimed for. Similar motion patterns were observed in alligators, both through direct observation and on videos, when the animals used their tails to strike at objects.

Several different versions of the whipping motion models were created, with shorter or longer 'handles', but since those with the shortest handle produce the highest speeds resembled the observed motions of extant crocodylians the most, and are osteologically feasible, only these motions are discussed here. Whiplash motions were modeled only as 'torque' models, using the simplified 5-segment version of the tail. Whiplash motions were also modeled without impacts on target, to determine if the stability of the pose was influenced by strikes missing the target.

Impact Forces

The pressure created by a spike impact on another animal depends on the mass and speed of the spike, which determine the impulse transferred, and on the stopping time, as well as the contact area. The impulse delivered to the target is

$$I_{spike} = m_{spike} * v_{impact} \quad (2),$$

and the maximum force exerted

$$F_{impact} = \frac{I_{spike}}{t} \quad (3).$$

Applied over a target area A this force creates a pressure P

$$P = \frac{F_{impact}}{A_{spiketip}} \quad (4),$$

where I_{spike} is the impulse of the spike, m_{spike} its mass, and v_{impact} its velocity at the time of impact, F_{impact} the force it can deliver, t the stopping time, and $A_{spiketip}$ the area of the spike tip that contacts the target.

For the sake of simplicity, the area of the spike tip is here assumed to be identical to that calculated for tail spikes of *Stegosaurus* by Carpenter et

al. (2005), 0.28 cm^2 , for penetrating strikes. Stopping time is difficult to estimate, and Carpenter et al. (2005) and Arbour (2009) use the conservative value of 0.33 s. Another example of high-energy collisions from the paleontological literature is head-butting behavior in pachycephalosaurs (Snively and Cox 2008). From the deceleration distances and speeds given in that publication, the implicitly assumed stopping time can be calculated, which varies between 0.018 s and 0.11 s for the average deceleration distance. However, these deceleration distances include not only the skull-skull collision, but additionally assume neck and potentially hindlimb motions (Snively and Cox 2008). For investigating a collision between a *Kentrosaurus* tail spike and, e.g., the skull or torso of a large theropod, it is impossible to estimate whether, and how, the target body would move or deform. However, data is available for a collision involving a relatively stiff element, somewhat similar to a tail spike, and a softer, deformable object, which can represent a bone/soft tissue complex: Tsaousidis and Zatsiorsky (1996) and Tol et al. (2002) give the time a football player's foot is in contact with the ball at around 0.016 s. Since force is inversely proportional to stopping time, using 0.016 s instead of 0.333 s as the stopping time means a ~21-fold increase in force, and thus pressure. Even shorter contact times of roughly 0.01 s are reported for football collisions in Australian rules football by Ball (2008), slightly higher values by Smith et al. (2009), who report an average of 0.022 s. What value should reasonably be used for calculating a tail-antagonist collision? Pachycephalosaurs appear to be adapted to cushioning impacts by flexion of the vertebral column (Carpenter 1997, figure 1), which are taken into account by Snively and Cox (2008), whereas a tail strike against a predator's flank could not be thus or similarly absorbed. Also, one must assume that in agonistic behavior, the participants have time to reposition their bodies and pretense muscles to maximize stopping time, while a predator probably did not have this chance when a stegosaur defended itself by tail strikes.

In bighorn sheep, deceleration takes place in less than 0.3 s (Kitchener 1988), again in a situation where there are shock-absorbing structures present that extend the stopping time (Farke 2008). Therefore, significantly shorter stopping times for the bone-bone collisions (spike with thin horn cover against skull, ribs, limbs near joints) investigated here appear reasonable, and 0.05 s is arbitrarily selected as the sole tested value. This

value is close to the average determined from Snively and Cox (2008), and thus probably too long, resulting in an underestimation of the impact forces at least for strikes hitting bone. Longer stopping times would certainly be created by collision with large amounts of soft tissue, but such tissues have much lower resistance to shear stress, so that comparable injuries would result.

RESULTS

Video material cited in the text can be found online.

palaeo-electronica.org/2011_2/255/video1.

palaeo-electronica.org/2011_2/255/video2.htm

palaeo-electronica.org/2011_2/255/video3.htm

Tail Musculature Reconstruction

The three CAD model versions of the tail used here have total muscle cross section areas per side at the base of the tail of 365 cm² ('slim' model), 615 cm² ('medium' model), and 1265 cm² ('croc' model). In comparison, the alligator sections scaled to the same bone dimensions show a larger muscle cross section area (1525 cm²) than even the 'croc' model. Calculated torque values available at the base of the tail vary between 542 Nm (specific tension 20 N/cm², 'slim' model) and 13047 Nm (specific tension 78 N/cm², 'croc' model). The 'medium' model delivers a range between 1112 Nm (20 N/cm²) and 4336 Nm (78 N/cm²).

Mass Estimates and COM Position

The 'slim' CAD model has a total volume of 1073 L. The 'medium' tail model is 17 L larger, and the 'croc' tail model nearly 195 L. Soft tissue density can range from 0.3 kg/L for goose necks (Bramwell and Whitfield 1974) to 1.2 kg/L, depending on the anatomical part of the organism that is being measured, such as neck, tail, or thorax (e.g., Schmidt-Nielsen 1984, 1997; Anderson et al. 1985; Christiansen and Farina 2004). Compact bones, of which the tail spikes are almost exclusively constructed, weighs nearly 2 kg/L (Currey 2002). Generally, terrestrial animals have an overall density of roughly 1 kg/L, but values as high as 1.15 kg/L have been reported (Bellmann et al. 2005). Here, all body parts were given a density of 1 kg/L, except for the tail (1.25 kg/L). All values were varied in all model versions to account for slightly different soft tissue reconstructions. An adult *Kentrosaurus* is thus estimated to have weighed between slightly over 1 t to 1.5 t. Different distribu-

tions of the osteoderms showed a similar shift in COM position as variations of density in different body parts. Overall, as long as the volume of soft tissues was varied within sensible borders in one segment (forelimbs, trunk, hindlimbs, or neck), the COM was not displaced by more than 0.05 m, except for a mass increase in the tail by 195 kg (switch from 'slim' to 'croc' model, which moved the COM 0.15 m posteriorly). The percentage of body weight supported on the hindlimbs varied between 70% and 94%, with most values in the 80-85% bracket. Varying the mass of the model outside the tail had no significant influence on the performance of the tail.

The COM showed only minimal lateral and craniocaudal motions for all tail deflection angles, with full 6° deflection leading to a maximal motion laterally of 0.086 m and 0.017 cm craniocaudally. Accelerations remained significantly under 0.5 g in all non-whiplash models, with maximum values of 0.63 g achieved in simple whip motions, in which the tail slammed into the motion limits of the joints unchecked. More complex whip models achieving higher speeds showed lateral accelerations below 0.2 g. There were no significant differences between the detailed and the simplified tail models.

Accelerations reached levels of ~ 7 g for impacts on a generic body of 750 kg that represents a mid-sized to large theropod. However, such models must be interpreted with caution, because the *Kentrosaurus* model is internally stiff, so that there is no cushioning of the impact at all, while in reality the tail itself would probably passively flex along the entire length to absorb the energy. Therefore, these models were no longer assessed.

Continuous Tail Swings

Tail tip speeds for continuous swings ranged between 3.34 m/s and 15.93 m/s, with the value for 5° deflection and 1.5 s swing time being 9.14 m/s. These motions resulted in a sinusoid torque curve in each joint, with the maximum value well below the possible maximum torques calculated for the corresponding muscle cross sections for swing times of 1.5 s and longer, and slightly above for 1 s swing times in the slim model. However, if the joint orientation is not prescribed via a sinusoid curve, but manually adjusted to create a more even torque input, torques of ~ 70% of the theoretical calculated maximum are sufficient to create 1 s swing times. The 'medium' and 'croc' models had sufficient muscle force available for 1 s swings as well. The linear momentum of the tail tip spike pair

Table 2. Continuous tail swings: Tail tip maximum velocities and linear momentum of the distal tail for different deflection angles and swing times.

swing time (s)	1	1	1	1.5	1.5	1.5	2	2	2
deflection per joint (°)	2.5	5	6	2.5	5	6	2.5	5	6
max speed (m/s)	6.7	13.74	15.93	4.46	9.14	11.05	3.34	6.83	8.25
Linear momentum (kgm/s)									
'slim', tail tip 10.7 kg	71.69	147	170.5	47.72	97.8	118.2	35.74	73.08	88.28
'medium', tail tip 11.8 kg	79.06	162.1	191.2	52.63	107.9	130.4	39.41	80.59	97.35
'croc', tail tip 14.85 kg	99.50	204	191.2	66.23	135.7	164.1	49.6	101.4	122.5

ranges between 35.74 kgm/s and 191.2 kgm/s (Table 2). Values for the 'medium' and 'croc' models are 10% and 39% greater, respectively, than those of the 'slim' model, due to the greater mass.

Whiplash Tail Swings

Whiplash motions (Video 1, Video 2, and Video 3) achieve significantly higher speeds than continuous swings. The least muscular 'slim' model, at the lowest specific tension of 20 N/cm², reached speeds over 25 m/s, and covered an arc of over 50° at a speed over 10 m/s (Figure 6.1). The 'medium' model reached 39 m/s at this specific tension (Figure 7.1, Video 2). All other combinations of muscle reconstructions with specific tension values tested achieved at least 40 m/s (Figures 6.2-6.4, 7, 8, Video 3, Table 3). The 'croc' model at a specific tension of 78 N/cm² reaches 100 m/s, and covers an arc of over 120° at over 10 m/s, and an arc of nearly 100° at over 20 m/s (Figure 8.4).

Impact Forces

At a tail tip weight of 10.7 kg with one tail tip spike pair, the 'slim' model can exert a pressure of over 3800 N/cm² at speeds as low as 5 m/s for a strike with a 0.28 cm² tip of a spike. At 8 m/s the impact exceeds the failure parameters of the frontal region of the human skull, which is between 4448 N/cm² and 6200 N/cm² (Ono et al. 1980), for a 0.28 cm² spike tip, and at 20 m/s and 25 m/s for a 1 cm² tip. At 20 m/s the pressure would be over 15 kN/cm² for a 0.28 cm² tail tip area. This is close to the shear stress of cortical bone as listed by Carpenter et al. (2005), but significantly higher than the various values given by Currey (2002). An impact at 40 m/s impact velocity might push the spike tip so deep into the target body that bones a significant distance from the surface could come into contact with the spike tip, e.g., caudal vertebrae. Even across a 10 cm² impact area, which corresponds to a penetration depth of nearly 30

cm, a pressure of nearly 1 kN/cm² would have been available.

These calculations assume that a spike tip impacts at a steep angle. At other angles the contact area would be potentially much larger, and the resulting pressure much lower, but the volume of affected tissue accordingly larger. The 'medium' and 'croc' model tail tips are slightly heavier, due to a slightly larger amount of soft tissues, and accordingly achieve slightly higher impact forces.

Hennig (1925) and Janensch (1925) envisaged the tail osteoderms as evenly distributed, with one pair of terminal spikes. If there were two closely spaced pairs of spikes on the distal tail end as in *Stegosaurus* (Carpenter 1998), the impact forces would be significantly increased by the much larger mass of the tail tip. Accelerations, however, would be only minimally smaller, because the added mass of a second spike pair is negligible compared to the mass of the entire tail. Similarly, if the contact time was greater due to a reduced deceleration of the impacting spike, e.g. when impacting on soft tissues or on a body part with very thin bones (e.g., a skull), a larger part of the distal tail could contribute its impulse to the collision, further increasing the pressure.

DISCUSSION

Tail Musculature Reconstruction

Of the three musculature cross section reconstructions used here the 'slim' model (Figures 4.1, 5.1-5.3) is comparable to the classic bone-delimited models used, e.g., by Carpenter et al. (2005) and Arbour (2009), and the simple elliptical model of Allen et al. (2009), with the bone sized 22% of the muscle cross section area. The 'medium' model has 14% bone surface area, and the 'croc' model has 7.5%, close to the value determined for *Alligator* (Figure 4.2-4.3). The latter model lies within the variations for soft tissue extents of the accurate models of Allen et al. (2009). Inspection

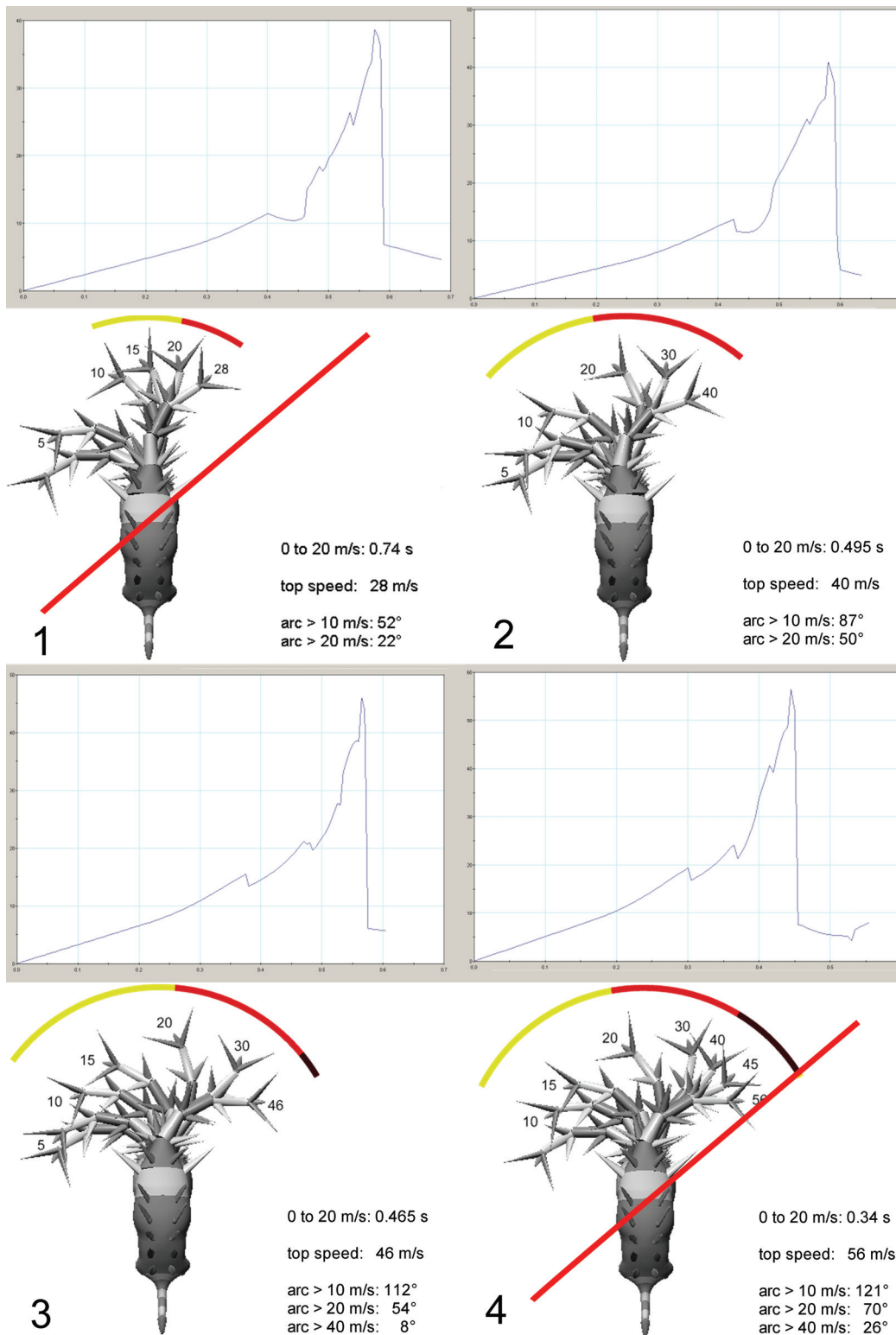


Figure 6. Modeling results of the 'slim' model. In each figure part the graph gives speed of the tail tip (m/s) versus time (s), and superimposed dorsal views of the model show position of the tail as given speeds of tail tip. Arc shows arcs covered by tail tip at speeds greater than 10 m/s, 20 m/s, 40 m/s, and 60 m/s. Time to accelerate to 20 m/s and top speed are given, as well as arcs covered above selected speeds. Specific tension is (1) 20 N/cm², (2) 39 N/cm², (3) 50 N/cm², and (4) 78 N/cm². Combinations of speed and muscle reconstruction deemed unrealistic are marked by a red diagonal line.

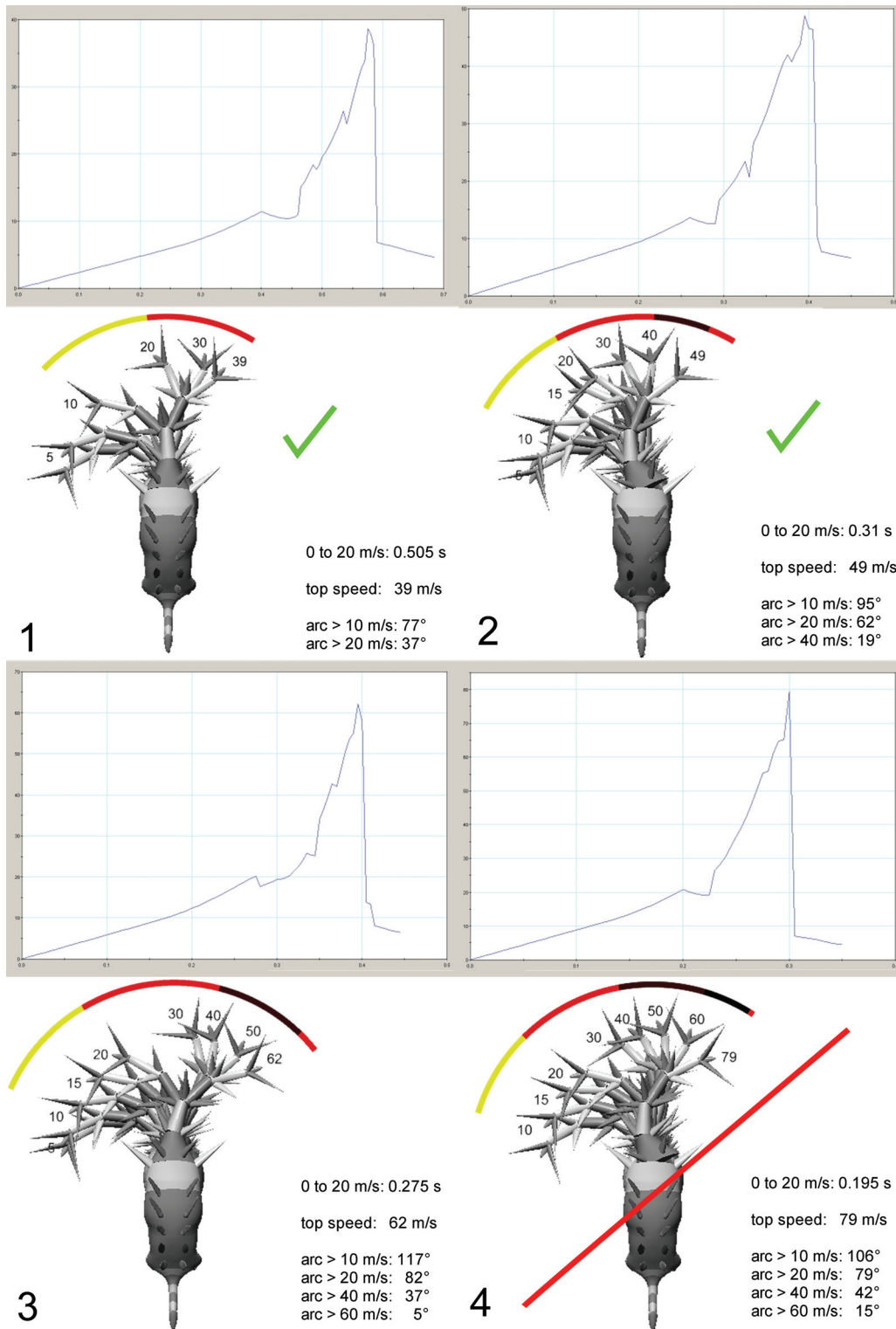


Figure 7. Modeling results of the 'medium' model. In each figure part the graph gives speed of the tail tip (m/s) versus time (s), and superimposed dorsal views of the model show position of the tail as given speeds of tail tip. Arc shows arcs covered by tail tip at speeds greater than 10 m/s, 20 m/s, 40 m/s, and 60 m/s. Time to accelerate to 20 m/s and top speed are given, as well as arcs covered above selected speeds. Specific tension is (1) 20 N/cm², (2) 39 N/cm², (3) 50 N/cm², and (4) 78 N/cm². Combinations of speed and muscle reconstruction deemed unrealistic are marked by a red diagonal line, and results in the best estimate bracket are marked by a green check mark.

Table 3. Whiplash tail swings: Swing times, tail tip maximum velocities, and linear momentum of the distal tail.

specific tension (N/cm ²)	slim		medium		croc	
	torque at base (Nm)	v _{max} (m/s)	torque at base (Nm)	v _{max} (m/s)	torque at base (Nm)	v _{max} (m/s)
20	542.8	28	1111.8	38	3345.4	42
39	1058.5	40	2168.0	49	6523.5	59
50	1357.0	46	2779.5	62	8363.5	69
78	2116.9	56	4336.0	80	13047.1	101

of X-ray and CT scans of various reptiles confirmed that normally, the soft tissues in the tail of healthy individuals extend beyond the bone by at least 15-20%, more often 30 to 40%, measured in dorsal view, similar to the values in the 'medium' model. In crocodiles and alligators, the muscles can extend to 190% of the bone structure laterally, while the rate in the dorsoventral axis is usually close to 130%. These results diverge somewhat from those of Allen et al. (2009), but may depend on individual variations of the specimens studied. The large amount of musculature on the tails of crocodiles may be connected to the fact that they use their tails for swimming.

In sum, the 'slim' model should be discounted as unrealistically conservative (see Allen et al. 2009, Persons 2009), possibly having only half the correct muscle cross sections. Calculations based on it suffer not only from unrealistically low muscle diameters and thus force estimates. Smaller muscles result in lower moment arms (see examples in Figure 4.1-4.3, 4.5). Because torque is the product of force and moment arm, torque estimates for the 'slim' models may be as low as 25% of the real value. The 'medium' model probably is the best conservative approximation, while a crocodile-like model may overestimate the muscle volume of *Kentrosaurus*. However, non-avian dinosaurs relied mainly on the m. caudofemoralis for locomotion (Gatesy 1990), so a large m. caudofemoralis and an accordingly large axial musculature should be expected. Because thyreophorans very likely used their tails as the primary means of defense (e.g., Carpenter et al. 2005), it is possible that their musculature was similarly or even more developed than that of extant crocodylians.

Mass Estimates, COM Position, and Motions

Kentrosaurus shows the typical COM position of quadrupedal dinosaurs, with the greater part of the weight supported by the hindlimbs. The percentage of weight supported by the hindlimbs is high for a quadruped at 80% to 85%, comparable to many basal and some derived sauropodo-

morphs (Henderson 2006; Mallison 2010b). For *Stegosaurus* a similar COM position was found by Henderson (1999), and the generally similar body proportions of other stegosaurs indicate that this pattern is true for the entire group. Due to the short moment arm from the COM to the hips, lateral acceleration of the entire body was probably easily effected, allowing rapid pivoting around the hind foot with relatively little exertion.

The large moment arm between the forelimb and the COM, combined with the high flexibility of the tail, lead to modest lateral accelerations of the anterior body in all CAE models. A stiff tail would induce a large amount of rotational inertia to the trunk if halted suddenly, but the tail of *Kentrosaurus* modeled here moves laterally only at its base. Continuous flexion along the tail means that the distal half is moving mostly anteriorly in relation to the animal's trunk just before reaching extreme deflection, so that the resulting transferred moment can easily be taken up in the forelimb. In none of the simulation runs it is necessary to broaden the stance in the forelimbs to increase the moment arm by choosing a sprawling posture to achieve stability. However, impacts of the tail on a very large (>200 kg) and thus inert target at high speeds tend to create large lateral accelerations, in some simulation runs achieving 7g laterally, which is sufficient to topple or laterally shift the model unless correcting motions were taken in the forelimbs or hindlimbs. These events require extreme forces in the shoulder and elbow. Under such circumstances a sprawling forelimb position would have been a significant aid in stabilizing the posture, explaining why the maximal forces in the shoulder and elbow were possibly not caused by locomotion. More detailed modeling of such impacts and target-missing tail swings will be needed to clarify the exact forces and accelerations involved.

Tail Swings

For the discussion of tail swings, the combination of the under-muscled 'slim' model and the lowest specific tension value, 20 N/cm² (Figure 6.1),

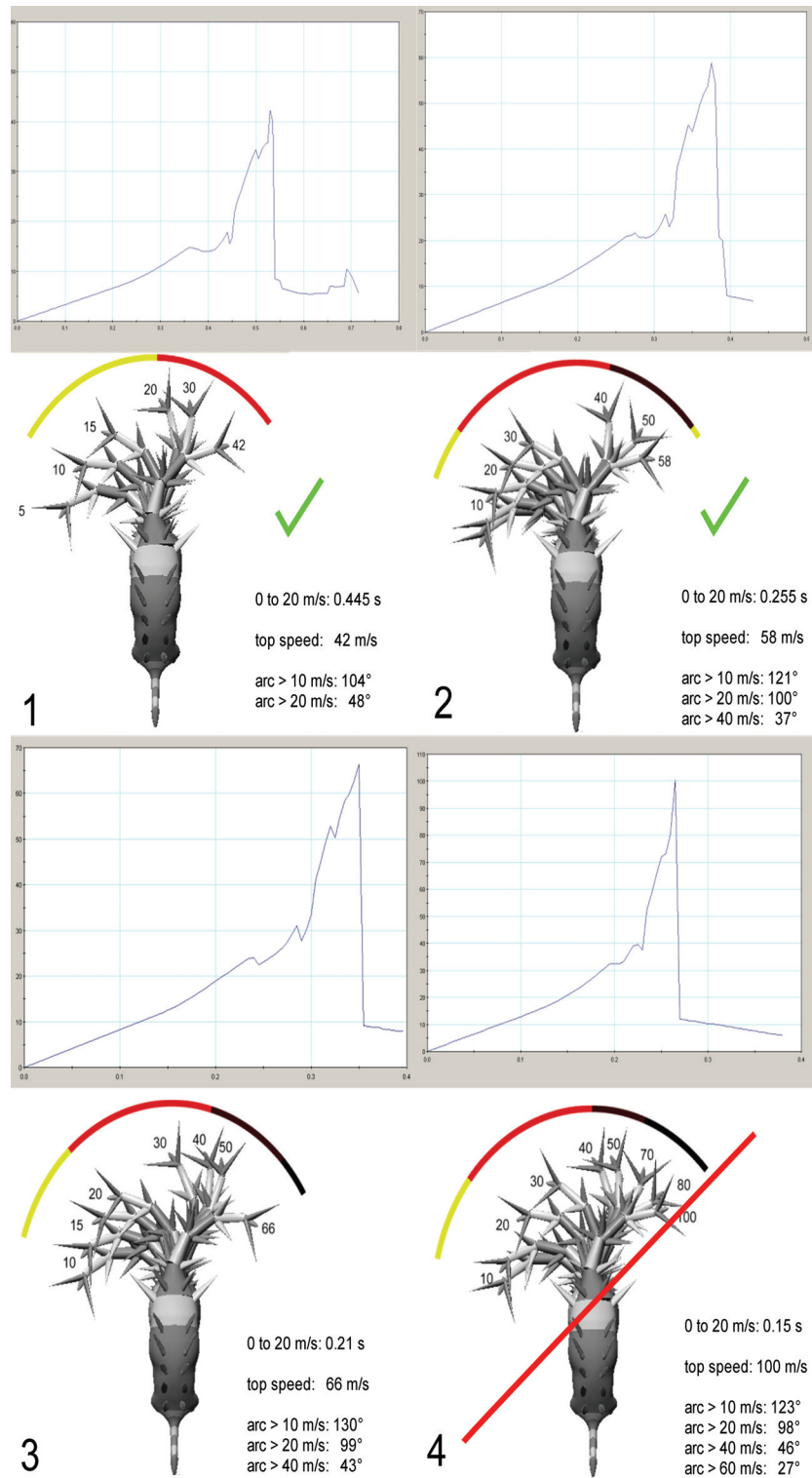


Figure 8. Modeling results of the 'croc' model. In each figure part the graph gives speed of the tail tip (m/s) versus time (s), and superimposed dorsal views of the model show position of the tail as given speeds of tail tip. Arc shows arcs covered by tail tip at speeds greater than 10 m/s, 20 m/s, 40 m/s, and 60 m/s. Time to accelerate to 20 m/s and top speed are given, as well as arcs covered above selected speeds. Specific tension is (1) 20 N/cm², (2) 39 N/cm², (3) 50 N/cm², and (4) 78 N/cm². Combinations of speed and muscle reconstruction deemed unrealistic are marked by a red diagonal line, results in the best estimate bracket are marked by a green check mark.

will be ignored, because it suffers from a multiplication of errors, not only addition (i.e., if half the correct moment arm is multiplied by half the correct force, the resulting torque will be only 25% of the true value), that make the final results unrealistic. The unrealistically low muscle cross section results in too low a calculated force, which is then multiplied with the moment arm that is also too low because of the anorexic reconstruction. Although a specific tension of 20 N/cm² is a realistic value, it is at the lower end of the range reported for muscles of larger animals, and thus cannot ameliorate the effect of the double error introduced by the 'slim' musculature reconstruction. Similarly, models using specific tension values greater than 50 N/cm² are discounted here as well (Figures 6.4, 7.4, 8.4), because recent experimental studies consistently find values below 60 N/cm². Although it is certainly possible that values between 50 N/cm² and 60 N/cm² as found by O'Brien et al. (2010) or values below 20 N/cm² (e.g., Maganaris et al. 2001) are also correct, using the 20–50 N/cm² range eliminates the highest and lowest extremes of the reliable values. The combinations of the 'medium' and the 'croc' model with a specific tension value of 20 N/cm² to 39 N/cm² are considered to provide the range of best estimates here.

All other models reach top speeds of at least ~ 40 m/s, and the arc covered at over 10 m/s is greater than 75° (Figures 6.2-6.3, 7.1-7.3, 8.1-8.3). Using the lowest specific tension value of 20 N/cm², the two realistic musculature reconstructions, the 'medium' and 'croc' models, arc greater than 90° at 10 m/s and nearly 40° above 20 m/s (Figures 7.1, 8.1). At this speed the spikes could penetrate deeply into soft tissues or between ribs and were able to shatter bones. Using 50 N/cm², these models top 60 m/s, arcing over more than 80° at over 20 m/s (Figures 7.3, 8.3). Impacts at this speed, creating localized pressure over 5 kN/cm², would have been sufficient to cause serious, likely fatal injury independent of the exact body part hit and the exact geometry of the impact, because the failure parameters of even relatively strong bones are exceeded (e.g., Ono et al. 1980). The best estimate models suggest top speeds between ~ 50 m/s and 55 m/s, and high speeds (> 20 m/s) across arcs greater than 60°.

Penetrating Impacts

Penetrating impacts at 10 m/s created forces greater than those sufficient to fracture a human skull (Ono et al. 1980), and thus were probably

hard enough to pierce integuments and fracture bones close to the surface such as ribs or some facial bones, the latter even of large theropods. At 20 m/s the impact energy was probably sufficient to drive the spikes deeper, despite the increasing diameter. Because the tail tip spikes of *Kentrosaurus* are very slender, their diameter increases little with increasing penetration depth, so that deeper penetration requires little additional force. The cross section area of importance is therefore that directly behind the apical diameter increase. Due to the flattened shape, the cross section area here is roughly 9 cm² in MB.R.3803 on both spikes (~ 10 cm² including a thin keratin layer), while those of the longer spikes mounted on the exhibition mount in the MFN (MB.R.4842 and 4843) are slightly larger, at 13 cm² and 13.5 cm², respectively. This means that the tail tip moving at 40 m/s, a value achieved as top speed by all realistic models and across a significant arc by the 'medium' model for a specific tension of 50 N/cm² and the 'croc' model for 39 N/cm², the spikes were able to crush bones equivalent to a human skull.

When striking the torso, however, the lance-like shape makes it likely that the spikes would slip on ribs and push through the intercostal musculature. Even below 20 m/s the models predict impact forces sufficient to cause deep penetration if only soft tissues are hit. Once the body wall of the trunk was perforated, the spikes could slip deeply into the lungs or intestines against little resistance, causing massive and probably lethal soft tissue damage. Strikes at the posterior end of the ribcage, where no sturdy girdle elements are in the way, and where ribs tend to be less stout in dinosaurs, would be especially effective. Probably even more dangerous were hits on the neck. Less deep, because of the slightly greater resistance of muscles, but still incapacitating injury probably occurred on the tail base (comparable to that of the *Allosaurus* caudal described by Carpenter et al. [2005]) and limbs.

As shown by Carpenter et al. (2005), penetrating strikes create a high risk that spikes become lodged in the target body and subjected to high bending moments. This possibility causes a high risk of fracture, even more so in the slimmer *Kentrosaurus* spikes than in the sturdier osteoderms of *Stegosaurus*.

Slashing Impacts

If the tips of the spikes were drawn across a predator's body, the effect would depend on the exact angle. If there were sufficient pressure, the

high speed and sharp tip would lead to gouging injuries, with the spike tip cutting into soft tissues and potentially fracturing thin, superficial bones. The keels on the spikes may indicate a keratin sheath that exaggerated the keels, making the outside shape more blade-like (H. Larsson, personal commun., 2010). However, the keels were proportionally small in tail spikes, and in the tail tip, spikes mostly are not ridges sticking out, but only sudden changes in curvature (Figure 3.2), so that this possibility remains speculative, and is ignored here.

Slashing hits are potentially lethal where large blood vessels run close to the surface of the body without being protected by thick bone, e.g., on the skull and neck. Sheet-like muscles such as the m. trapezius are at the risk of being totally severed, while thicker muscles can be harmed badly as well, so that loss of limb function is a realistic danger. Slashing impacts likely were rare, because the strike geometry requires that the target is at exactly the right distance to the stegosaur. A little further away and the tail misses, a little closer and the impact becomes a blunt strike. However, if such hits occurred, the calculated impact energies were certainly sufficient to cause dangerous wounds.

Blunt Impacts

Given the angled attachment of the spikes on the tail, this type of impact is the most likely. Among this category, those strikes must also be counted in which the tip of the spike initially penetrates, but at a shallow angle, so that almost immediately a large area comes into contact with the target.

Blunt strikes distribute the energy of the impact on a larger force than penetrating strikes, reducing the peak pressure. The larger the area, the lower the pressure on any specific point. The effective contact surface of a stegosaur tail spike may have been as large as half the total lateral aspect, roughly 120 cm² (Figures 1, 3). In a blunt strike, the spike would therefore not penetrate the integument. Instead, the spike would be brought to a halt in contact with the target's surface, transferring probably not only the kinetic energy of the tail tip, but that of the entire distal part of the tail. However, because the tail consists of not just one rigid block, but a system of links embedded in muscle, the deceleration would result in some internal motion. Combined with the absence of penetration this means that the contact time between spike and target would be relatively long, giving bones close to the surface time to break due to bending, not due to being crushed locally by a point impact.

In the interest of traffic safety, a number of studies have been performed in which impactors of various weights were used to cause blunt trauma in human cadavers at speeds typical for auto accidents, usually under 10 m/s. Viano et al. (1989) used a circular 23.4 kg impactor with a 177 cm² impacting surface at speeds of 4.5 m/s, 6.7 m/s and 9.4 m/s in lateral impacts, causing rib fractures and occasionally pubic ramus fractures. Talantikite et al. (1998) used smaller impactors (12 kg and 16 kg) of the same size and a narrower speed range (6 m/s to 8.5 m/s). During 11 tests on human cadavers they recorded between three and eight broken ribs, with between three and 16 separate fractures (Talantikite et al. 1998, table 5). Both studies also recorded occasional liver ruptures (Viano et al. 1989; Talantikite et al. 1998). Impacts of the 23.4 kg impactor at 9.4 m/s are roughly comparable to a 10 m/s blunt impact of a *Kentrosaurus*-tail tip spike, while those of the lighter impactors create lower forces on the thorax than a spike hit would. In summation, it is reasonable to assume that at least similar injuries occurred during tail impacts on targets with rib sizes similar to humans.

This means that even at modest speeds, the tail of *Kentrosaurus* could cripple small and medium-sized theropod no matter what angle the tail tip spikes impacted. Large predators with a thick integument probably suffered only minor injuries at low impact speeds. However, a doubling of the impact speed to 20 m/s means that the impact force is also doubled, while at 40 m/s the force is quadrupled, so that all tail strike models deemed realistic could cause multiple rib fractures even in large theropods. For example, the anterior dorsal ribs of the abelisaurid theropod *Majungasaurus crenatissimus* (Depéret, 1896) Lavocat, 1955 measure less than 30 mm across the base of the shaft (O'Connor 2007) and are thus less than four times as strong as human ribs, which have an average greatest shaft thickness of roughly 12 mm (e.g., Abrams et al. 2003). Other structures of similar robustness could also be broken by blunt strikes, such as scapula blades or facial bones.

Aside from breaking bony structures, the impact of a club can cause other potentially lethal injuries, e.g., the rupture of internal organs or blood vessels, or severe muscle damage. Strikes to the skull can result in concussions or intracranial lesions.

Tail Swing Times

Despite the threat to attackers posed by the tail, *Kentrosaurus* was apparently not immune to

attacks, especially by predators that were fleet of foot. Collision speeds are much lower near the base of the tail than at the tip, so that a quick dash just after the tail had passed could have allowed a predator to get close enough to the tail base to be safe from lethal or serious injury. A return of the tail on the reverse swing takes between 1 s and 4 s in the 'torque' models, depending on the applied torques, giving ample time for a well-timed sprint across the 3 m distance between the hips of *Kentrosaurus* and a safe spot just outside the tail's reach. Also, the tail covered only the posterior aspect, so that the anterior body and neck were unprotected (Mallison 2010a). Of this area, as much as 90° may have been covered at speeds sufficient to cause lethal injury ('croc' model, 50 N/cm², Figure 8.3). However, this means that three quarters of the stegosaur were exposed to attacks unless the animal reacted timely to a threat and rotated the entire body so that the 'danger zone' of possible high tail speeds faced the threat. Defensive action thus required a good overview of the immediate surroundings. The 360° circumferential visibility required a maximally extended and thus vulnerable neck, while lateral flexion of the neck resulted in a large dead area created by the body (Mallison 2010a). In any case, rapid pivoting of the entire body was required to bring the tail to bear, facilitated by the extremely posterior COM position.

An important point about the times for strikes calculated here is that the tail is already in a maximally lateroflexed position at the beginning, thus positioned for a full-power strike. Another advantage of this prepositioning is that it allows the muscles of the extended side that will have to perform the strike to be maximally stretched. The passive part of the muscles' force production curve can thus be used to generate a high torque and rapid acceleration quickly. Essentially, part of the force required to perform a rapid strike can be delivered by the muscles of the contralateral side of the tail and stored in the stretched muscles. Extant monitor lizards and crocodylians sometimes prepare for defensive action in this way. Komodo dragons (*Varanus komodensis*) occasionally even run away holding their tails off the ground and strongly lateroflexed and strike at pursuers when they come into range (pers. obs.). The time to preposition the tail must be added to the times calculated here if an attempt is made to judge the time interval between two swipes of the tail, i.e., the time window available to a predator to get close.

Comparison to Previous Works

A comparison of the results presented here to those of Carpenter et al. (2005) and Arbour (2009) is difficult. The torque values calculated here are significantly higher than those found by Carpenter et al. (2005) for *Stegosaurus* and Arbour (2009) for ankylosaurs, due to the extremely low estimates of muscle cross sections in these studies. However, because Carpenter et al. (2005) and Arbour (2009) incorrectly used the half-width of the reconstructed tail, represented by the distance between the horizontal tail midline and tip of the transverse process, the assumed moment arms do not conform to the musculature reconstructions, and may in fact be close to the actual values (see Figure 4 on moment arm position versus muscle size), so that the overall error in Carpenter et al.'s and Arbour's calculations is much smaller than that of the 'slim' model used here. Additionally, Carpenter et al. (2005) miscalculated several values, resulting in a roughly 10-fold increase of the estimated pressure at impact in their *Method 1* (Carpenter et al. 2005, p.336), and used an incorrect physical formula (*Pressure* is defined as *Impulse per Area* instead of *Force per Area*, Carpenter et al. 2005, p. 340). Also, the motion range of the tail was estimated very low, with an average limit of below 2.5° per intervertebral joint (Carpenter et al. 2005, p. 340) between osteoderm plates and total rigidity assumed within segments (Carpenter et al. 2005, p.338, contra *ibid*, figure 17.6a). Illustrations of *Stegosaurus* caudals in Marsh (1880), Gilmore (1914), and Galton and Upchurch (2004) and personal inspection of mounted skeletons in the NMS and DMNS do not indicate a significantly reduced lateral mobility compared to *Kentrosaurus*. Carpenter (1998, figure 5a) showed a hypothetical *Stegosaurus* tail without osteoderms at maximum flexion, in an overall curve generally similar to that found for *Kentrosaurus* at 5° by Mallison (2010a). Larger amount of soft tissues than assumed by Carpenter (1998) and Carpenter et al. (2005) would allow more motion, and it is also not clear why mobility should be possible in only one single joint, and not a group of two or three joints at the overlap points of osteoderm plates. Biomechanically, such a system with no motion in most joints and significant motion in one single joint should lead to differing joint morphologies, which are not visible on any known skeleton.

SUMMARY

The tail of *Kentrosaurus* probably had a large motion arc covering the entire half-circle behind the animal (Mallison 2010a). Modeling results indicate that it could swing across most of this arc with sufficient speed to cause serious injury. Muscle force estimates at the unrealistic lower end of the spectrum reported here result in moderate impact speeds and impact forces. Such hits certainly smarted, comparable to the hits large extant monitors distribute with their tails (e.g., Holland 1915). More muscular and realistic models of *Kentrosaurus* achieve speeds at which impacts could seriously harm predators. Without whiplash motion, speeds of approximately 5-14 m/s could likely be achieved for the tail tip, depending on the specific tension of the musculature assumed. In the case of spike tip hits with an intact horn cover, as envisaged by Carpenter et al. (2005) for *Stegosaurus* sand with the impact angle close to 90°, at these speeds the tail spike tips could very likely penetrate soft tissues deeply, and fracture thin bones such as ribs or facial bones. Collisions with larger contact areas, e.g. the side of a spike, at any significant speed would result at least in the typical injuries resulting from blunt trauma with moderate energy, such as concussions, large hematomas, and crush injuries. Simulations of simple tail swings using the largest musculature reconstruction, the 'croc model', suggest that a hit squarely on a predator's skull may well have been sufficient to maim or kill even without whiplash motions.

Whiplash motion models indicate high tail tip velocities and thus impact forces for relatively low accelerating and decelerating torques. Large arcs could be covered at speeds greater than 20 m/s, and top speeds of ~ 40 m/s appear realistic. The risk of the tail damaging itself when hitting osteological stops seems minimal due to the motion geometry. Whiplash strike simulations predict impact forces easily sufficient to cause critical injuries on predators of all sizes. Within the arc covered by the whiplash swing of the tail tip at speed greater 40 m/s, which is small compared to the total motion range of the tail but may have amounted one quarter of the animal's aspect, strikes probably could cause lethal deep penetrating trauma to the head, neck, and torso of even large predators. For small- to medium-sized (< 200 kg) theropods even impact speeds of 20 m/s or less were potentially lethal, due to the large inertia of the tail tip. Blunt trauma of the skull was likely incapacitating, while internal organs may have

been less affected, although a strike against the ribcage would likely have resulted in multiple rib fractures.

An aimed blow required exact timing of the impact in both space and time. At slow swing speeds (2 s), a near miss would invite a predator to step into the arc, exposing the tail base and pelvic region to bites. The swing speeds and tail tip speeds sustained across large arcs, however, suggest that such an attack strategy was risky, because realistic models predict swing times much lower than 1 s, and times to accelerate the tail tip to speeds sufficient to cause serious injury at below 0.5 s. Return strikes may have been possible in less than 2-4 s. Overall, modeling results suggest that *Kentrosaurus* was capable of defending itself effectively against any single threat, so that coordinated attacks by two or more predators may have been required to endanger the animal.

ACKNOWLEDGMENTS

The idea for this study was originally hatched in a discussion with K. Carpenter (Denver Museum of Nature and Science), to whom I am also much indebted for showing me, before publication, the original "thagomized" *Allosaurus* vertebra. H.-J. 'Kirby' Siber and the crew of the SMA organized and invited me to their highly productive Stegosaur Meeting, for where an initial report on this study was given. Their effort and enthusiasm has greatly aided the study of stegosaurus, and I am deeply indebted to them. J.R. Hutchinson and V. Allen (Royal Veterinary College) both greatly aided my understanding of biomechanics, for which I am very grateful, as well as for their comments on a draft of this manuscript. H.-U. Pfretzschner (Eberhard-Karls-University Tübingen) discussed tail swings with me repeatedly, greatly helping my understanding of underlying mechanics of tail motions. Reviews of a previous version of the manuscript by P. Galton (University of Bridgeport) and an anonymous reviewer, and of this version by H. Larsson (Redpath Museum, McGill University) greatly improved the manuscript.

REFERENCES

- Abrams, E., Mohr, M., Engel, C., and Bottlang, M. 2003. Cross-sectional geometry of human ribs. *American Society of Biomechanics, Conference Abstracts 2003*. Retrieved from <http://www.asbweb.org/conferences/2003/pdfs/196.pdf>.
- Alexander, R.M. 1989. *Dynamics of Dinosaurs and Other Extinct Giants*. Columbia University Press, New York.

- Alexander, R.M., Farina, R.A., and Vizcaino, S.F. 1999. Tail blow energy and carapace fractures in a large glyptodont (Mammalia, Xenarthra). *Zoological Journal of the Linnean Society*, 126:41-49.
- Allen, V., Paxton, H., and Hutchinsin, J.R. 2009. Variation in center of mass estimates for extant sauropsids and its importance for reconstructing inertial properties of extinct archosaurs. *Anatomical Record*, 292:1442-1461.
- Anderson, J., Hall-Martin, A., and Russel, D. 1985. Long bone circumference and weight in mammals, birds and dinosaurs. *Journal of Zoology*, 207:53-61.
- Arbour, V.M. 2009. Estimating impact forces of tail club strikes by ankylosaurid dinosaurs. *PLoS ONE* 4:e6738. doi:10.1371/journal.pone.0006738.
- Bakker, R.T. 1986. *The Dinosaur Heresis*. William Morrow and Co., New York.
- Ball, K. 2008. Foot interaction during kicking in Australian rules football, p. 36-40. In Reilly, T. and Korkusuz, F. (eds.), *Science and football VI* (pp. 36-40). Routledge, London.
- Barmé, M. 1964. *Kraft, Ermüdung und elektrische Aktivität der Kaumuskelatur und der Flexoren am Oberarm*. M.D. thesis, University of Cologne, Cologne.
- Bellmann, A., Suthau, T., Stoinski, S., Friedrich, A., Hellwich, O., and Gunga, H. 2005. 3D modelling of dinosaurs. In Grün, A. and Kahmen, H. (eds.), *Optical 3-D Measurement Techniques VII (Proceedings of the 7th Conference) Part 1*. Vienna.
- Bernstein, B., Hall, D.A., and Trent, H.M. 1958. On the dynamics of a bull wip. *Journal of the Acoustical Society of America*, 30:1112-1115.
- Bottinelli, R. and Reggiani, C. 2000. Human skeletal muscle fibres: molecular and functional diversity. *Progress in Biophysics and Molecular Biology*, 73:195-262.
- Bramwell, C.B. and Whitfield, G.R. 1974. Biomechanics of *Pteranodon*. *Philosophical Transactions of the Royal Society of London, Series B*, 267:503-581.
- Carpenter, C.C. 1961. Patterns of social behavior in the desert iguana, *Dipsosaurus dorsalis*. *Copeia*, 1961:396-405.
- Carpenter, K. 1997. Agonistic behavior in pachycephalosaurs (Ornithischia: Dinosauria): a new look at head-butting behavior. *Contributions to Geology, University of Wyoming*, 32:19-25.
- Carpenter, K. 1998. Armor of *Stegosaurus stenops*, and the taphonomic history of a new specimen from Garden Park Colorado. *The Upper Jurassic Morrison Formation: An Interdisciplinary Study. Part 1. Modern Geology*, 22:127-144.
- Carpenter, K., Sanders, F., McWhinney, L.A., and Wood, L. 2005. Evidence for predator-prey relationships. Examples for *Allosaurus* and *Stegosaurus*, p. 325-350. In Carpenter, K. (ed.), *The Carnivorous Dinosaurs*. Indiana University Press, Bloomington.
- Christiansen, P. 1996. The "whiplash" tail of diplodocid sauropods: was it really a weapon?, p. 51-58. In Morales, M. (ed.), *The Continental Jurassic*. Museum of Northern Arizona Bulletin.
- Christiansen, P. and Farina, R.A. 2004. Mass prediction in theropod dinosaurs. *Historical Biology*, 16:85-92.
- Clutton-Brock, T. 1982. The function of antlers. *Behaviour*, 79:108-125.
- Cong, L., Hou, L., Wu, X., and Hou, J. 1998. *The gross anatomy of Alligator sinensis Fauvel*. Forestry Publishing House, Beijing.
- Coombs, W.P. 1978. Forelimb muscles of the Ankylosauria (Reptilia, Ornithischia). *Journal of Paleontology*, 52:642-657.
- Coombs, W.P. 1979. Osteology and myology of the hindlimb in the Ankylosauria (Reptilia, Ornithischia). *Journal of Paleontology*, 53:666-683.
- Currey, J.D. 2002. *Bones: Structure and Mechanics*. Princeton University Press, New Jersey.
- Daudin, F.M. 1802. *Histoire Naturelle, Générale et Particulière des Reptiles; ouvrage faisant suit à l'Histoire naturelle générale et particulière, composée par Leclerc de Buffon; et rédigée par C.S. Sonnini, membre de plusieurs sociétés savantes*. Vol. 2. F. Dufart, Paris
- Delp, S.L. and Loan, J.P. 1995. A graphics-based software system to develop and analyze models of musculoskeletal structures. *Computers in Biology and Medicine*, 25:21-34.
- Delp, S.L. and Loan, J.P. 2000. A computational framework for simulating and analyzing human and animal movement. *Computing in Science and Engineering*, 2:46-55.
- Depéret, C. 1896. Sur l'existence de dinosaurien sauropodes et théropodes dans le Crétacé supérieur de Madagascar. *Comptes Rendus de l'Académie des Sciences, Paris*, 122:483-485.
- Dong, Z., Tang, Z., and Zhou, S.W. 1982. [Note on the new Mid-Jurassic stegosaur from Sichuan Basin, China]. *Vertebrata Palasiatica* 20:83-87. (In Chinese)
- Farke, A.A. 2008. Frontal sinuses and head-butting in goats: a finite element analysis. *Journal of Experimental Biology*, 211:3085-3094.
- Fick, R. 1911. Anatomie und Mechanik der Gelenke unter Berücksichtigung der bewegenden Muskeln. In *Handbuch der Anatomie des Menschen, 2. Bd., Abt. 1, Teil 1-3*. Gustav Fischer Verlag, Jena.
- Fox, L. 1962. *Numerical Solution of Ordinary and Partial Differential Equations*. Addison-Wesley, Oxford.
- Franke, F. and Bethe, A. 1919. Beiträge zum Problem der willkürlich beweglichen Armprothesen, IV, Kraftkurven. *Münchener medizinische Wochenschrift*, 66:201-205.
- Frey, E., Riess, J., and Tarsitano, S.F. 1989. The axial tail musculature of recent crocodiles and its phyletic implications. *American Zoologist*, 29:857-862.

- Galton, P.M. and Upchurch, P. 2004. Stegosauria, p. 343-362. In Weishampel, D.B., Dodson, P., and Osmolska, H. (eds.), *The Dinosauria, 2nd Edition*. University of California Press, Berkeley.
- Gasc, J. 1981. Axial musculature, p. 355-435. In Gans, C. and Parsons, T.S. (eds.), *Biology of the Reptilia, vol. II*. Academic Press, London.
- Gatesy, S.M. 1990. Caudofemoral musculature and the evolution of theropod locomotion. *Paleobiology*, 16:170-186.
- Geist, V. 1971. *Mountain Sheep*. Chicago University Press, Chicago.
- Gilmore, C.W. 1914. Osteology of the armored Dinosauria in the United States National Museum, with special reference to the genus *Stegosaurus*. *United States National Museum Bulletin*, 89:1-136.
- Henderson, D.M. 1999. Estimating the masses and centers of mass of extinct animals by 3D mathematical slicing. *Paleobiology*, 25:88-106.
- Henderson, D.M. 2006. Burly gaits: centers of mass, stability and the trackways of sauropod dinosaurs. *Journal of Vertebrate Paleontology*, 26:907-921.
- Hennig, E. 1915. *Kentrosaurus aethiopicus*, der Stegosauride des Tendaguru. *Sitzungsberichte der Gesellschaft naturforschender Freunde zu Berlin*, 1915:219-247.
- Hennig, E. 1925. *Kentrurosaurus aethiopicus*. Die Stegosaurier-Funde vom Tendaguru, Deutsch-Ostafrika. *Palaeontographica*, 2 Supplement 7:101-254.
- Holland, W.J. 1915. Head and tails: a few notes relating to the structure of sauropod dinosaurs. *Annals of the Carnegie Museum*, 9:273-278.
- Hutchinson, J.R., Anderson, F.C., Blemker, S., and Delp, S.L. 2005. Analysis of hindlimb muscle moment arms in *Tyrannosaurus rex* using a three-dimensional musculoskeletal computer model: implications for stance, gait, and speed. *Paleobiology*, 31:676-701.
- Ikai, M. and Fukunaga, T. 1968. Calculation of muscle strength per unit cross-sectional area of human muscle by means of ultrasonic measurement. *Internationale Zeitschrift für Angewandte Physiologie*, 26:26-32.
- Janensch, W. 1925. Ein aufgestelltes Skelett des Stegosauriers *Kentrurosaurus aethiopicus* Hennig 1915 aus den Tendaguru-Schichten Deutsch-Ostafrikas. *Palaeontographica*, 2 Supplement 7:255-276.
- Kitchener, A.C. 1988. An analysis of fighting of the blackbuck (*Antilope cervicapra*) and the bighorn sheep (*Ovis canadensis*) and the mechanical design of the horns of bovids. *Journal of Zoology*, 214:1-20.
- Langenberg, W. 1970. Morphologie, physiologischer Querschnitt und Kraft des M. erector spinae in Lumbalbereich des Menschen. *Zeitschrift für Anatomie und Entwicklungsgeschichte*, 132:158-190.
- Lavocat, R. 1955. Sur une portion de mandible de théropode provenant du Crétacé supérieur de Madagascar. *Bulletin du Muséum National d'Histoire Naturelle, Série 2*, 27:3.
- Lull, R.S. 1910. *Stegosaurus unguulatus* Marsh, recently mounted at the Peabody Museum of Yale University. *American Journal of Science, 4th Series*, 30:361-377.
- Maganaris, C.N., Baltzopoulos, V., Ball, D., and Sargeant, A.J. 2001. In vivo specific tension of human skeletal muscle. *Journal of Applied Physiology*, 90:865-872.
- Maidment, S.C.R., Wei, G., and Norman, D.B. 2006. Re-description of the postcranial skeleton of the Middle Jurassic stegosaur *Huayangosaurus taibaii*. *Journal of Vertebrate Paleontology*, 26:944-956.
- Maleev, E.A. 1952. [A new ankylosaur from the Upper Cretaceous of Asia]. *Doklady Akademii Nauk S.S.S.R*, 87:273-276. (In Russian)
- Mallison, H. 2010a. CAD assessment of the posture and range of motion of *Kentrosaurus aethiopicus* Hennig 1915. *Swiss Journal of Geosciences*, 103:211-233. doi:10.1007/s00015-010-0024-2.
- Mallison, H. 2010b. The digital *Plateosaurus* I: body mass, mass distribution, and posture assessed using CAD and CAE on a digitally mounted complete skeleton. *Palaeontologia Electronica* 13.2.8A. palaeo-electronica.org/2010_2/198/index.html
- Mallison, H. 2011. The real lectotype of *Kentrosaurus aethiopicus* Hennig 1915. *Neues Jahrbuch für Geologie und Paläontologie*.
- Marsh, O.C. 1877a. Notice of new dinosaurian reptiles from the Jurassic formation. *American Journal of Science and Arts*, 14:514-516.
- Marsh, O.C. 1877b. A new order of extinct Reptilia (Stegosauria) from the Jurassic of the Rocky Mountains. *American Journal of Science*, 14:513-514
- Marsh, O.C. 1880. Principal characters of American Jurassic dinosaurs, Part III. *American Journal of Science, 3rd Series*, 19:253-259.
- Marx, J.O., Olsson, M.C., and Larsson, L. 2006. Scaling of skeletal muscle shortening velocity in mammals representing a 100,000-fold difference in body size. *Pflügers Archiv - European Journal of Physiology*, 452:222-230. doi:10.1007/s00424-005-0017-6.
- Mateus, O., Maidment, S.C., and Christiansen, N.A. 2009. A new long-necked 'sauropod-mimic' stegosaur and the evolution of the plated dinosaurs. *Proceedings of the Royal Society B: Biological Sciences*, 276:1815-1821. doi:10.1098/rspb.2008.1909.
- McWhinney, L.A., Rothschild, B.M., and Carpenter, K. 2001. Posttraumatic chronic osteomyelitis in *Stegosaurus* dermal spikes, p. 141-156. In Carpenter, K. (ed.), *The Armored Dinosaurs*. Indiana University Press, Bloomington.
- Milstead, W.W. 1970. Late summer behavior of the lizards *Sceloporus merriami* and *Urosaurus ornatus* in the field. *Herpetologica*, 26:343-354.
- Myhrvold, N.P. and Currie, P.J. 1997. Supersonic sauropods? Tail dynamics in diplodocids. *Paleobiology*, 23:393-403.

- O'Brien, T.D., Reeves, N.D., Baltzopoulos, V., Jones, D.A., and Maganaris, C.N. 2010. In vivo measurement of muscle specific tension in adults and children. *Experimental Physiology*, 95:202-210.
- O'Connor, P.M. 2007. The postcranial axial skeleton of *Majungasaurus crenatissimus* (Theropoda: Abelisauridae) from the Late Cretaceous of Madagascar. *Journal of Vertebrate Paleontology*, 27:127-162.
- Ono, K., Kikuchi, A., Nakamura, M., Kobayashi, H., and Nakamura, N. 1980. Human head tolerance to sagittal impact. Reliable estimation deduced from experimental head injury using subhuman primates and human cadaver skulls. *25th Stapp Car Crash Conference Proceedings, Warrendale, Pennsylvania* 101-160.
- Paul, G.S. 1987. The science and art of restoring the life appearance of dinosaurs and their relatives. A rigorous how-to guide., p. 5-49. In Czerkas, S.J. and Olson, E.C. (eds.), *Dinosaurs Past and Present Volume II*. Natural History Museum of Los Angeles County Press, Los Angeles.
- Persons, W. 2009. Theropod tail muscle reconstruction and assessment of the locomotive contributions of the M. caudofemoralis. *Journal of Vertebrate Paleontology*, 29 Supplement to No.3:164A.
- Pooley, A.C. and Gans, C. 1976. The Nile crocodile. *Scientific American*, 234:114-124.
- Roberts, S.C. 1996. The evolution of hornedness in female ruminants. *Behaviour*, 133:399-442.
- Romer, A.S. 1923a. Crocodilian pelvic muscles and their avian and reptilian homologues. *Bulletin of the American Museum of Natural History New York*, 48:533-552.
- Romer, A.S. 1923b. The pelvic musculature of sauropsid dinosaurs. *Bulletin of the American Museum of Natural History New York*, 48:605-617.
- Romer, A.S. 1927. The pelvic musculature of ornithischian dinosaurs. *Acta Zoologica*, 8:225-275.
- Schmidt-Nielsen, K. 1984. *Scaling: Why Is Animal Size So Important?* Cambridge University Press, Cambridge.
- Schmidt-Nielsen, K. 1997. *Animal Physiology: Adaptation and Environment*. Cambridge University Press, Cambridge.
- Smith, J., Ball, K., and MacMahon, C. 2009. Foot-to-ball interaction in preferred and non-preferred leg Australian rules kicking, 650-653. In Anderson, R., Harrison, D., and Kenny, I. (eds.), *ISBS - Conference Proceedings Archive, 27th International Conference on Biomechanics in Sports 2009*. University of Limerick, Limerick.
- Snively, E. and Cox, A. 2008. Structural mechanics of pachycephalosaur crania permitted head-butting behavior. *Palaeontologia Electronica* 11.1.3A.
- Talantikite, Y., Bouguet, R., Rarnet, M., Guillernot, H., Robin, S., and Voiglio, E. 1998. Human thorax behaviour for side impact - Influence of impact mass and velocities. *Proceedings of the Conference on the Enhanced Safety of Vehicles*, 1998:98-S7-O-03.
- Tol, J.L., Slim, E., van Soest, A.J., and van Dijk, C.N. 2002. The relationship of the kicking action in soccer and anterior ankle impingement syndrome: A biomechanical analysis. *American Journal of Sports Medicine*, 30:45-50.
- Tsaousidis, N. and Zatsiorsky, V. 1996. Two types of ball-effector interaction and their relative contribution to soccer kicking. *Human Movement Science*, 15:861-876.
- Viano, D.C., Lau, I.V., Asbury, C., King, A.I., and Bege-man, P. 1989. Biomechanics of the human chest, abdomen, and pelvis in lateral impact. *Accident Analysis and Prevention*, 21:553-574. doi:10.1016/0001-4575(89)90070-5.
- Winter, S.L. and Challis, J.H. 2003. Estimating the specific tension of muscle in vivo: a simulation study, p. 2. In *American Society of Biomechanics Annual Conference 2003*. Presented at the American Society of Biomechanics, Toldeo, Ohio. Retrieved from <http://www.asbweb.org/conferences/2003/pdfs/213.pdf>.